Privacy-Preserving Platooning Control of Vehicular Cyber–Physical Systems With Saturated Inputs

Dengfeng Pan, Derui Ding, *Senior Member, IEEE*, Xiaohua Ge, *Senior Member, IEEE*, Qing-Long Han, *Fellow, IEEE*, and Xian-Ming Zhang, *Senior Member, IEEE*

***Abstract*—Metaverse allows the physical reality to tightly integrate with the digital universe. As one typical metaverse application, platooning control of vehicular cyber–physical systems has attracted extensive attention as it is beneficial to improve traffic efficiency, driving safety, and emission reduction. However, due to the open nature of wireless communication networks, the transmitted vehicle-to-vehicle (V2V) data packets become exposed to the public and concomitant data leakage can lead to unintended consequences to vehicular platoons. This article is concerned with the privacy-preserving platooning control issue of vehicular cyber–physical systems with input saturations. First, a novel distributed proportional-integral observer is proposed to estimate the full state of each vehicle, where the integral terms with a forgetting factor facilitate to realize the tradeoff between transient performance and steady-state performance for the platoon. Second, sampled-data-based dynamic encryption and decryption schemes, featuring a dynamic private key, are developed such that the encrypted and decrypted V2V data can be kept private to each platoon vehicle. It is then shown that the platooning control problem over a generic communication topology can be cast into the stability issue of an auxiliary dynamic system. Furthermore, sufficient conditions on the existence of the desired observer and controller gains as well as the private key parameter selection are derived to guarantee the desired platoon stability and privacy preservation requirements. Finally, an illustrative example is given to demonstrate the effectiveness of the proposed control method.**

***Index Terms*—Encryption and decryption, platooning control, privacy preservation, proportional-integral observers (PIOs), vehicular cyber–physical systems.**

I. Introduction

INDUSTRY 5.0 is regarded as a cornerstone of future industrial development. Metaverse, an emerging technology that aims to build a decentralized virtual world, is put up within the context of Industry 5.0. So far, industrial manufacturers and researchers are working on bringing a seamless connection between the real and virtual world to our daily life, and fruitful results about the application of Metaverse in automobile industries have been reported; see [1], [2], [3], [4], [5], [6], and [7] and references therein. Those results show the potential of Metaverse to improve vehicle performance and the driver's experience. However, Metaverse applications in connected and automated vehicles rely heavily on suitable wireless communication networks to guarantee safety both in the real and cyber worlds [8], [9], [10], [11], [12]. Therefore, how to better integrate communication networks with physical vehicles, leading to the so-called vehicular cyber–physical system, is of both theoretical and practical significance. Among the various control problems for vehicular cyber–physical systems, platooning control, whose primary objective is to coordinate a group of connected and automated vehicles such that they can travel in close proximity to one another at highway speeds, has attracted intensive attention; see the recent surveys [13], [14], [15], [16]. In their early stage, vehicles mainly use onboard sensing devices such as radars and lidars to get information from other vehicles. As a result, vehicles can only obtain information from the vehicles nearest to them, and the developed platooning control results apply to only the predecessor-following platoon structure. With the rapid development of communication and network technologies, the vehicle-to-vehicle (V2V) information flow topologies become much more flexible and versatile, under which the platooning control performance can generally be made better [17], [18], [19].

Metaverse aims to provide customized services to its users, requiring unique data from different users. Benefitting from the flourishing telecommunication and automotive industries, vehicles have the ability to share information with various remote transportation participants via different networks, including V2V communication networks, vehicle-to-infrastructure communication (V2I) networks, and vehicle-to-everything (V2X) communication networks [20]. Along with the advantage of information exchanges, there is an ever-increasing concern about data leakage due to the open nature of communication networks [21], [22], [23], [24], [25]. As such, data privacy is regarded as a critical issue that should be taken into consideration in vehicle platooning control. Up to now, data leakage has been an urgent yet under-appreciated problem. From the perspective of system security, any leaked data leaves the system vulnerable to cyber attacks as malicious adversaries are very likely to launch more targeted attacks [26], [27], [28]. Vehicles suffering from those malicious attacks may collide with their preceding or following vehicles. Fortunately, the problem of data privacy

Manuscript received 3 November 2022; accepted 25 November 2022. Date of publication 19 December 2022; date of current version 17 March 2023. This work was supported in part by the Australian Research Council Discovery Early Career Researcher Award under Grant DE200101128. This article was recommended by Associate Editor F.-Y. Wang. *(Corresponding author: Qing-Long Han.)*

The authors are with the School of Science, Computing and Engineering Technologies, Swinburne University of Technology, Melbourne, VIC 3122, Australia (e-mail: qhan@swin.edu.au).

Color versions of one or more figures in this article are available at https://doi.org/10.1109/TSMC.2022.3226901.

Digital Object Identifier 10.1109/TSMC.2022.3226901

This work is licensed under a Creative Commons Attribution 4.0 License. For more information, see https://creativecommons.org/licenses/by/4.0/

preservation has stimulated scientific interest in the past few years. To date, several cryptographic techniques, such as block chain [21], [22], group signatures [23], trustworthiness evaluation [24], and voting theory [25], have been applied to vehicular platoon privacy preservation. At the same time, various proactive defense mechanisms of moving targets have been developed to improve the system security, see the survey [29]. It should be pointed out that these cryptographic techniques require high computation resources. In vehicle platooning control, such a drawback is intolerable to manufacturers as it will lead to a cost surge. Additionally, these cryptographic techniques only focus on logical data privacy and overlook their impacts on platoon control performance.

Apart from the cryptographic techniques, the communication network itself also plays an important role in the privacy problem. For instance, a 5G-based V2X communication network is proposed in [30] to guarantee the privacy requirements of data where the communication task is allocated to the proper network slice. Moreover, the notion of ϵ-differential privacy is also prevalent in the field of data privacy preservation. When considering ϵ-differential privacy, Laplacian or Gaussian noises will be added to the original data such that each data can not be recognized uniquely while keeping the overall statistic characteristics of the data almost unchanged. Although ϵ-differential privacy can put system dynamics into consideration, these added noises may cover the original data and destroy the data integrity. One of the effective approaches to overcome such a shortage is to add fading noises to the original data [31], [32], [33]. However, these added noises will still deviate the system from the desired consensus states [31]. Even worse, the ϵ-differential privacy mechanism will lose its effectiveness as the added noises decay to zero. Motivated by the k-anonymity in private data release technology [34], [35], this article aims to design a privacy-preserving control scheme based on the output of vehicles and eliminate the adverse effects of the privacy-preserving scheme.

Up to now, various state-feedback controllers have been proposed for vehicular cyber–physical systems in [17], [18], and [36]. However, in many practical situations, the full state of a vehicle may not be measured directly and precisely. Therefore, it is necessary to develop suitable observers to estimate the full states of vehicles via leveraging the limited sensor measurements. In comparison with traditional Luenberger observers, proportional-integral observers (PIOs) provides additional degrees of freedom to improve the estimated performance via an additional integral term. Specifically, such degree of freedom can eliminate the steady-state estimation errors and becomes more robust to disturbances or uncertainties [37], [38]. Nevertheless, the employed integral term inevitably impairs the transient performance of PIOs. It then becomes important to realize the tradeoff between transient performance and steady-state performance. Furthermore, considering both privacy-preserving schemes and PIOs, it is also nontrivial to develop an easy-to-implement scheme to design the desired controller and observer gains while finding the verifiable condition on the parameters of privacy-preserving schemes.

Summarizing the discussion above, this article presents a distributed PIO-based control scheme with a privacy-preserving guarantee for a class of vehicular cyber–physical systems subject to input saturations. The main contributions of this article are highlighted as follows.

1) A novel PIO with a forgetting factor in the integral term is constructed to estimate the full states of vehicles while realizing the tradeoff between transient performance and steady-state performance.
2) A distributed encryption–decryption-based platooning control law is developed for each following vehicle. The proposed encryption and decryption schemes feature a dynamic private key that plays a key role in preserving the privacy of each vehicle's data.
3) By resorting to nonsingular transformation as well as the special structure of vehicular platoon systems with a digraph, the issue of platooning control is transformed into the stability issue of an auxiliary system.
4) Sufficient conditions on the existence of the desired PIOs and platoon controllers are derived to guarantee the expected platoon stability and privacy-preserving performance. It is shown that the selected range of parameters in private keys can be explicitly disclosed.

The remainder of this article is arranged as follows. Section II presents the preliminaries and formulates the main problem to be solved. Section III provides the main results in terms of stability analysis and gain design of PIOs and controllers. An illustrative example is given in Section IV to verify the effectiveness of the derived main results. Conclusions are drawn in Section V.

Notations: $\mathbb{N}$ denotes the set of natural numbers, and $\mathbb{N}^+$ stands for the set $\mathbb{N}/\{0\}$. For symmetric matrix X, $X < 0$ means that X is negative definite. $A^\top$ and $\lambda(A)$ are the transpose and the eigenvalue of matrix A. $\lambda_{\max}(A)$ ($\lambda_{\min}(A)$) denotes the maximum (minimum, respectively) eigenvalue. $\text{diag}\{A_1, A_2, \ldots\}$ means a block-diagonal matrix whose diagonal elements are $A_1, A_2, \ldots$ "**e**" describes Euler's number. Other notations are quite standard except where otherwise stated.

II. Preliminaries and Problem Formulation

A. V2V Communication Topologies

Consider a vehicular platoon encompassing one leader and N followers. The V2V communication topology among followers can be described by a digraph $\mathcal{G} = \{\mathcal{V}, \mathcal{E}, \mathcal{A}\}$ with the node set $\mathcal{V} = \{1, 2, \ldots, N\}$, the edge set $\mathcal{E} = V \times V$, as well as the adjacency matrix $\mathcal{A} = [a_{ij}] \in \mathbb{R}^{N\times N}$. A directed edge (i, j) belongs to $\mathcal{E}$ with $a_{ij} = 1$ if and only if there is a communication link from j to i; $(i, j) \notin \mathcal{E}$ and $a_{ij} = 0$, otherwise. Furthermore, vehicular j is regarded as a neighbor of vehicular i if $a_{ij} = 1$, and the neighbor set of node i is denoted as $\mathcal{N}_i = \{j \in \mathcal{V} : (i, j) \in \mathcal{E}\}$. Moreover, $\mathcal{L} = \mathcal{D} - \mathcal{A}$ denotes the Laplacian matrix of $\mathcal{G}$, where $\mathcal{D} = \text{diag}\{\sum_{j\in\mathcal{N}_1} a_{1j}, \sum_{j\in\mathcal{N}_2} a_{2j}, \ldots, \sum_{j\in\mathcal{N}_N} a_{Nj}\}$. Let $a_{i0} = 1$ for any $i \in \mathcal{V}$ if the ith vehicle can receive the information of the leader, and denote the pinning matrix as $\mathcal{D}_0 = \text{diag}\{a_{10}, a_{20}, \ldots, a_{N0}\}$.

Assumption 1: The directed graph $\mathcal{G}$ contains a spanning tree.

Assumption 2: The eigenvalues of $\mathcal{L}+\mathcal{D}_0$ are positive and real scalars.

Remark 1: Assumptions 1 and 2 are mild in the context of platooning control. Specifically, the spanning tree requirement holds for the commonly used information flow topologies, such as predecessor following (PF), predecessor leader following (PLF), bidirectional (BD), and BD leader (BDL). Furthermore, the eigenvalues of $\mathcal{L}+\mathcal{D}_0$ for those four topologies are all real. What is more, by the Gershgorin circle theorem, we know that the ith eigenvalue is located in $0 < \lambda_i(\mathcal{L}+\mathcal{D}_0) \leq \max_i\{\sum_{j\in\mathcal{N}_i} a_{ij}\}$ for $i = 1, 2, \ldots, N$.

B. Longitudinal Vehicle Dynamics

The widely studied third-order position–velocity–acceleration model [18], [39] is adopted to describe the longitudinal dynamics of each platoon vehicle

$$\tau \dddot{p}_i(t) + \ddot{p}_i(t) = u_i(t), \ \ i \in \mathcal{V} \tag{1}$$

where $p_i(t) \in \mathbb{R}$ is the position of vehicle i, $\tau \in \mathbb{R}$ is the inertial lag of longitudinal vehicle dynamics, and $u_i(t) \in \mathbb{R}$ denotes the desired acceleration control input to be designed. Similarly, the dynamics of the leader can be modeled by

$$\tau \dddot{p}_0(t) + \ddot{p}_0(t) = 0 \tag{2}$$

where $p_0(t) \in \mathbb{R}$ is the position of the leader. For simplicity, the control input is set as $u_0(t) = 0$. Introducing the augmented state $x_i(t) = [p_i(t), \dot{p}_i(t), \ddot{p}_i(t)]^T$ and the low-dimensional sensor measurement $y_i(t) \in \mathbf{R}^q$ with $q \leq 3$, the longitudinal dynamics (1) can be rewritten into the following state-space form:

$$\begin{cases} \dot{x}_i(t) = Ax_i(t) + Bu_i(t) \\ y_i(t) = Cx_i(t) \end{cases} \tag{3}$$

for $i \in \{0\}\cup\mathcal{V}$, where C is a known output matrix with full-row rank, and

$$A = \begin{bmatrix} 0 & 1 & 0 \\ 0 & 0 & 1 \\ 0 & 0 & -\frac{1}{\tau} \end{bmatrix}, \ B = \begin{bmatrix} 0 \\ 0 \\ \frac{1}{\tau} \end{bmatrix}.$$

Remark 2: One of the most important concepts of Metaverse is digital twins [6], [7]. Digital twins, a 2-tuple consisting of one digital entity and its corresponding entity in the real world, provides a novel insight into the integration of the virtual and real worlds. With such a virtual entity, we can describe and predict the behavior of its corresponding real entity. Therefore, it is necessary to investigate the behavior of virtual entities to guarantee a better performance of corresponding real entities. In what follows, leveraging only each vehicle's sensor measurement $y_i(t)$, we aim to develop a distributed observer and a distributed encryption–decryption-based controller in the virtual world. The virtual world will output the desired control input commands $u_i(t)$ for each vehicle $i \in \mathcal{V}$ in the physical world such that the platoon vehicles' longitudinal motions can be regulated in a distributed manner.

C. Distributed PIOs and Encryption–Decryption Schemes

For each vehicle $i \in \mathcal{V}$ in the platoon, the following distributed PIO is adopted to estimate its full state $x_i(t)$:

$$\begin{cases} \dot{\tilde{x}}_i(t) = A\tilde{x}_i(t) + Bu_i(t) \\ \qquad\quad + L_P(y_i(t) - \tilde{y}_i(t)) + L_I r_i(t) \\ \dot{r}_i(t) = -\phi r_i(t) + y_i(t) - \tilde{y}_i(t) \\ \tilde{y}_i(t) = C\tilde{x}_i(t) \end{cases} \tag{4}$$

where $\tilde{x}_i(t)$ and $\tilde{y}_i(t)$ describe, respectively, the estimates of state $x_i(t)$ and measurement $y_i(t)$, and $r_i(t)$ stands for the auxiliary variable to reflect the behavior of integral loops. The scalar $\phi > 0$ is the forgetting factor to balance the influence of historical data, and L_P and L_I are proportional and integral gains to be determined later.

Denoting the estimation error as $e_{oi}(t) = x_i(t) - \tilde{x}_i(t)$ and applying (4) to (3) lead to

$$\dot{e}_{oi}(t) = (A - L_P C)e_{oi}(t) - L_I r_i(t). \tag{5}$$

Then, defining $\psi_i(t) = [e_{oi}^\top(t), r_i^\top(t)]$, one has the following error dynamics:

$$\dot{\psi}_i(t) = \mathcal{A}_o \psi_i(t) \tag{6}$$

where $\mathcal{A}_o = \begin{bmatrix} A - L_P C & -L_I \\ C & -\phi I_q \end{bmatrix}$.

The observer's information $\chi_i(t) = [\tilde{x}_i^\top(t), r_i^\top(t)]^\top$ generally needs to be transmitted to its neighbors to realize the desired platooning performance. Considering privacy preservation [40], [41], [42], [43], we are now ready to construct the following encryption and decryption schemes. Let T be the sampling period of the transmitted data.

The following distributed sampled-data-based dynamic encryption scheme is proposed for each vehicle i:

$$\begin{cases} \xi_i(0) = 0 \\ \dot{\xi}_i(t) = \mathcal{A}_c \xi_i(t), \ \ t \in \big(kT, \ (k+1)T\big) \\ \Delta_i((k+1)T) = q\left(\dfrac{\chi_i\big((k+1)T\big) - \mathbf{e}^{\mathcal{A}_c T}\xi_i(kT)}{g\big((k+1)T\big)}\right) \\ \xi_i((k+1)T) = \mathbf{e}^{\mathcal{A}_c T}\xi_i(kT) \\ \qquad + g\big((k+1)T\big)\Delta_i\big((k+1)T\big) \end{cases} \tag{7}$$

with $\mathcal{A}_c = \begin{bmatrix} A & L_I \\ \mathbf{0} & -\phi I_q \end{bmatrix}$, where $\xi_i(t)$ is an internal state of encryptor i, $g(t)$ is a piecewise function serving as a dynamic encryption key with the following rule:

$$g(t) = \begin{cases} g_0\gamma^k, & t = kg_1T, k \in \mathbb{N} \\ g(kg_1T), & t \in (kg_1T, (k+1)g_1T) \end{cases} \tag{8}$$

where $g_0 > 0$, $g_1 \in \mathbb{N}^+$, and $\gamma \in (0, 1)$. The uniform quantizer $q(x)$ is defined as

$$q(x) = \begin{cases} d\hbar, & x \in \left(\left(d - \frac{1}{2}\right)\hbar, \left(d + \frac{1}{2}\right)\hbar\right) \\ -q(-x), & x \in \left(-\infty, -\frac{1}{2}\hbar\right) \end{cases}$$

with $d \in \{1, 2, 3, \ldots, M\}$ where $\hbar$ is a given quantizer level, and the overall range is $[-M\hbar, \ M\hbar]$.

For the received information $\Delta_j((k+1)T)$ from its neighbor j, the following distributed sampled-data-based decryption scheme is carried out:

$$\begin{cases} \hat{x}_{ij}(0) = 0 \\ \dot{\hat{x}}_{ij}(t) = \mathcal{A}_c \hat{x}_{ij}(t), \ t \in \big(kT, \ (k+1)T\big), \\ \hat{x}_{ij}((k+1)T) = e^{\mathcal{A}_c T} \hat{x}_{ij}(kT) \\ \quad\quad + g((k+1)T)\Delta_j((k+1)T) \end{cases} \tag{9}$$

where $\hat{x}_{ij}^\top(t)$ is an internal state of decryptor i for decrypting data from its neighbor j. According to (7) and (9), it is easy to verify that $\hat{x}_{ij}(t) = \xi_j(t)$.

The state $\xi_i(t)$ of encryptor i and $\hat{x}_{ij}^\top(t)$ of decryptor i can be, respectively, decomposed into $[\xi_{ix}^\top(t), \xi_{ir}^\top(t)]^\top$ and $[\hat{x}_{ijx}^\top(t), \hat{x}_{ijr}^\top(t)]^\top$ for the following presentation of controller design, where $\xi_{ix}(t) \in \mathbb{R}^3$ and $\hat{x}_{ijx}^\top(t) \in \mathbb{R}^3$ correspond to the estimated states, and $\xi_{ir}(t) \in \mathbb{R}^q$ and $\hat{x}_{ijr}^\top(t) \in \mathbb{R}^q$ correspond to the auxiliary variables.

D. Distributed Platooning Control Law

A *traditional* platooning control law with saturation constraints takes the following form:

$$u_i(t) = \mathrm{Sat}\left(K \sum_{j\in\mathcal{N}_i} a_{ij}\big(x_i(t) - x_j(t) - d_{ij}\big) + K a_{i0}(x_i(t) - x_0(t) - d_{i0})\right) \tag{10}$$

where K is the control gain to be designed, d_{ij} is the desired distance between the ith and jth vehicles, d_{i0} is the desired distance between the ith vehicle and the leader, and $\mathrm{Sat}(\cdot)$ is the saturation function to guarantee physical limits or safety requirements. Inspired by the method in [44], a dead-zone function $\Psi(t)$ is employed to deal with the challenge of saturation constraints, that is

$$\mathrm{Sat}(s) = s - \Psi(s) \tag{11}$$

where

$$\Psi(s) = \begin{cases} s - u_{\max}, & s > u_{\max} \\ 0, & -u_{\max} < s < u_{\max} \\ s + u_{\max}, & s < -u_{\max} \end{cases} \tag{12}$$

with $u_{\max}$ being the saturation level. Such a dead-zone function satisfies the following condition.

Lemma 1 [44]: There exists a positive scalar $\iota \in (0, 1)$ such that $\iota s^\top s \geq \Psi^\top(s)\Psi(s)$.

Due to privacy-preserving requirements, the encrypted data, rather than plain data of any platoon vehicle, will be sent to its neighboring vehicles via the communication network. To this end, the *actual* platooning control law should incorporate the encrypted and decrypted vehicular data. By virtue of the state of the encryptor and the output of the decryptor, we propose the following distributed platooning control law for each vehicle $i \in \mathcal{V}$:

$$u_i(t) = \mathrm{Sat}\big(\tilde{u}_i(t)\big) \tag{13}$$

with

$$\tilde{u}_i(t) = K \sum_{j\in\mathcal{N}_i} a_{ij}\big(\xi_{ix}(t) - \hat{x}_{ijx}(t) - d_{ij}\big) + K a_{i0}\big(\xi_{ix}(t) - \hat{x}_{i0x}(t) - d_{i0}\big).$$

Noting that $\xi_j(t) = \hat{x}_{ij}(t)$, one has that (13) is equivalent to

$$u_i(k) = \mathrm{Sat}\Bigg(K \sum_{j\in\mathcal{N}_i} a_{ij}\big(\xi_{ix}(t) - \xi_{jx}(t) - d_{ij}\big) + K a_{i0}(\xi_{ix}(t) - \xi_{0x}(t) - d_{i0})\Bigg). \tag{14}$$

Remark 3: In our encryption scheme, only $\Delta_i(kT)$ is transmitted via V2V communication networks. The dynamic encryption key is private to each vehicle and the data privacy is preserved. On the other hand, input saturation is a common phenomenon in vehicle platooning control owing to the physical limitations on throttles and brakes of each vehicle. The saturation nonlinearity is generally handled by transforming it into other smooth functions [45], [46], such as hyperbolic tangent and sigmoid functions. However, it is not an easy-to-implement tool for controller design due to the intrinsic nonlinearity of employed functions. Inspired by the approach in [44] and [47], a dead-zone function is employed to realize platooning control design.

To proceed with, we define the platoon tracking error as

$$e_{vi}^p(t) = p_i(t) - p_0(t) - d_{i0}$$
$$e_{vi}^v(t) = v_i(t) - v_0(t), \ e_{vi}^a(t) = a_i(t) - a_0(t).$$

Then, denoting $e_{vi}(t) = [e_{vi}^p(t), \ e_{vi}^v(t), \ e_{vi}^a(t)]^\top$ and $z_i(t) = \xi_{ix}(t) - \tilde{x}_i(t)$, recalling (3) and (14), one has

$$\begin{aligned} \dot{e}_{vi}(t) = &A e_{vi}(t) + BK \sum_{j\in\mathcal{N}_i} a_{ij}\big(e_{vi}(t) - e_{vj}(t)\big) \\ &+ BK \sum_{j\in\mathcal{N}_i} a_{ij}\big(z_i(t) - z_j(t)\big) \\ &- BK \sum_{j\in\mathcal{N}_i} a_{ij}\big(e_{oi}(t) - e_{oj}(t)\big) \\ &+ BK a_{i0}(z_i(t) - e_{oi}(t) + e_{vi}(t)) \\ &- BK a_{i0}(z_0(t) + e_{o0}(t)) - B\Psi(\tilde{u}_i(t)). \end{aligned}$$

For the simplicity of analysis, we further denote the following stacked vectors:

$$\begin{aligned} e_v(t) &= \left[e_{v1}^\top(t), e_{v2}^\top(t), \ldots, e_{vN}^\top(t)\right]^\top \\ e_o(t) &= \left[e_{o1}^\top(t), e_{o2}^\top(t), \ldots, e_{oN}^\top(t)\right]^\top \\ x(t) &= \left[x_1^\top(t), x_2^\top(t), \ldots, x_N^\top(t)\right]^\top \\ \tilde{u}(t) &= \left[\tilde{u}_1^\top(t), \tilde{u}_2^\top(t), \ldots, \tilde{u}_N^\top(t)\right]^\top \\ z(t) &= \left[z_1^\top(t), z_2^\top(t), \ldots, z_N^\top(t)\right]^\top \end{aligned}$$

and reorganize the above error dynamics as follows:

$$\begin{aligned} \dot{e}_v(t) = &((\mathcal{L} + \mathcal{D}_0) \otimes BK)z(t) - ((\mathcal{L} + \mathcal{D}_0) \otimes BK)e_o(t) \\ &- ((\mathcal{L} + \mathcal{D}_0) \otimes BK)(\mathbf{1}_N \otimes (z_0(t) + e_{o0}(t))) \\ &+ (I_N \otimes A + (\mathcal{L} + \mathcal{D}_0) \otimes BK)e(t) \\ &- (I_N \otimes B)\Psi(\tilde{u}(t)). \end{aligned} \tag{15}$$

On the other hand, there exists a nonsingular matrix Γ such that $\Gamma(\mathcal{L} + \mathcal{D}_0)\Gamma^{-1} = J$ with $J = \mathrm{diag}\{J_1, J_2, \ldots, J_m\}$, where J_i $(i = 1, 2, \ldots, m)$ is a Jordan matrix corresponding to the eigenvalue λ_i of $\mathcal{L} + \mathcal{D}_0$. For ease of development, set $\lambda_1 \leq \lambda_2 \leq \cdots \leq \lambda_m$. Furthermore, introduce new variables

$$\begin{aligned}\bar{e}_v(t) &= (\Gamma \otimes I_3)e_v(t), \quad \bar{r}(t) = \left(\Gamma \otimes I_q\right)r(t)\\ \bar{e}_o(t) &= (\Gamma \otimes I_3)e_o(t), \quad \bar{z}(t) = (\Gamma \otimes I_3)z(t)\\ \bar{e}_{o0}(t) &= (\Gamma \otimes I_3)e_{o0}(t), \quad \bar{z}_0(t) = (\Gamma \otimes I_3)z_0(t)\\ \bar{\Psi}(\tilde{u}(t)) &= (\Gamma \otimes I_3)\Psi(\tilde{u}(t)).\end{aligned}$$

One has

$$\begin{aligned}\dot{\bar{e}}_v(t) = &(I_N \otimes A + J \otimes BK)\bar{e}_v(t) + (J \otimes BK)\bar{z}(t)\\ &- (J \otimes BK)\bar{e}_o(t) - (I_N \otimes B)\bar{\Psi}(\tilde{u}(t))\\ &- (J \otimes BK)(\mathbf{1}_N \otimes (\bar{z}_0(t) + \bar{e}_{o0}(t))). \qquad (16)\end{aligned}$$

The objective of this article is to achieve the desired platooning requirement with the predetermined gap reference by designing a distributed PIO-based controller $u_i(t)$ (13) (or 14) under the encryption and decryption schemes (7)–(9). In other words, the purpose is to determine the gain matrices L_P, L_I and K such that the following two requirements are satisfied simultaneously.

O1: The estimation error (6) of the distributed PIO (4) is convergent exponentially, that is, $\|e_{oi}(t)\| \leq \tilde{\chi}(e_o(t))\mathbf{e}^{\vartheta^* t}$, where $\tilde{\chi}(\cdot)$ is a positive scalar function and $\vartheta^* < 0$ is a positive scalar.

O2: The platoon tracking error (15) (or 16) converges to zero, that is, $\lim_{t\to\infty}\|\bar{e}_v(t)\| = 0 \ \ \forall i \in \mathcal{V}$.

III. Stability Analysis and Controller Design

This section will design suitable gain matrices while deriving a sufficient condition to guarantee the stability of the PIO error dynamics. In light of the designed PIO, the control gain under the adopted privacy preserving framework will be further determined to ensure successful vehicle platooning.

We first examine the privacy of the employed encryption and decryption schemes. The variable $z_i(t) = \xi_{ix}(t) - \tilde{x}_i(t)$ describes the privacy-preserving error (i.e., the gap the protected data and the real ones). Then, denote the quantization error at time instant kT as

$$\delta_i(kT) = \Delta_i(kT) - \frac{\chi_i(kT) - \mathbf{e}^{\mathcal{A}_c T}\xi_i((k-1)T)}{g(kT)}.$$

Furthermore, it follows from the above formula and the fourth formula in (7) that:

$$\begin{cases} z_i((k+1)T) = \left[I_3, 0_{3\times q}\right]g((k+1)T)\delta_i((k+1)T)\\ z_i(0) = -\tilde{x}_i(0).\end{cases}$$

Lemma 2 [34]: For any $k \in \mathbb{N}$, one has

$$\|z(kT)\| \leq b(kT) \qquad (17)$$

where $b(t) = b_0\hbar\sqrt{3N}g(t)$ with $b_0 = \max\{(1/2), (1/\sqrt{3}g_0)\}$.

Remark 4: It is clear from the above lemma that the privacy-preserving error $z(kT)$ highly depends on both the dynamic private key $g(t)$ and the quantizer level $\hbar$, which are private to the public involving adversaries. In other words, the adversaries executing the encryption algorithm with unmatched parameters cannot infer the estimated value $\tilde{x}_i(t)$ of interested vehicle i via the eavesdropped data $\Delta_i(kT)$. Furthermore, the key $g(t)$ has the capability of improving quantitative accuracy via amplifying the quantizer's input.

A. Stability Analysis and PIO Gain Design

This section presents a sufficient condition for observer gain design, while guaranteeing the desired stability of the PIO error dynamics.

Theorem 1: Consider the distributed PIO (4) for vehicle i modeled by (3). The estimation error (6) is convergent exponentially if there exist positive definite matrices Q_1 and Q_2 and matrices $\tilde{L}_P$ and $\tilde{L}_I$ such that

$$\Xi_1 = \begin{bmatrix} Q_1A + A^\top Q_1 + \tilde{L}_P C + C^\top\tilde{L}_P^\top & \tilde{L}_I + C^\top Q_2\\ * & -2\phi Q_2\end{bmatrix} < 0$$

holds. Furthermore, the observer gain matrices are determined by $L_P = Q_1^{-1}\tilde{L}_P$ and $L_I = Q_1^{-1}\tilde{L}_I$.

Proof: Select the following Lyapunov candidate:

$$V_o(t) = \psi_i^\top(t)Q\psi_i(t), \qquad (18)$$

where $Q = \text{diag}\{Q_1, Q_2\}$.

Taking the derivation of (18) along error dynamics (6) results in

$$\dot{V}_o(t) = \psi_i^\top\left(Q\mathcal{A}_o + \mathcal{A}_o^\top Q\right)\psi_i(t).$$

Considering the relationship $\tilde{L}_P \triangleq Q_1L_P$ and $\tilde{L}_I \triangleq Q_1L_I$, one has that there exists a negative constant $\vartheta = \lambda_{\max}(\Xi_1)$ such that

$$\dot{V}_o(t) < \vartheta\psi_i^\top(t)\psi_i(t) \leq \frac{\vartheta}{\lambda_{\max}(Q)}V_o(t) \qquad (19)$$

if $\Xi_1 < 0$ holds.

Integrating both sides of (19) leads to

$$V_o(t) \leq V_o(0)\mathbf{e}^{\frac{\vartheta}{\lambda_{\max}(Q)}}$$

which, together with (18), means

$$\|e_{oi}(t)\| + \|r_i(t)\| \leq \sqrt{\frac{V_o(0)}{\lambda_{\min}(Q)}}\mathbf{e}^{\frac{\vartheta}{2\lambda_{\max}(Q)}t} \qquad (20)$$

that is, $e_{oi}(t)$ and $r_i(t)$ converge to zero exponentially. The proof completed. ■

B. Some Important Lemmas for Performance Analysis

This section is to provide two lemmas for subsequent controller design.

Lemma 3: For continuous function $h(t)$ satisfying $\lim_{t\to\infty} h(t) = 0$ and $|h(0)| < \infty$, one has

$$\lim_{t\to\infty}\int_0^t |e^{-a(t-\tau)}h(\tau)|d\tau = 0 \qquad (21)$$

where a is a positive scalar.

Proof: This lemma can be proved by the following two cases.

Case a): $\lim_{t\to\infty}\int_0^t |e^{a\tau}h(\tau)|d\tau < \infty$.

In this case, it is not difficult to find that

$$\lim_{t\to\infty}\int_0^t |e^{-a(t-\tau)}h(\tau)|d\tau = \lim_{t\to\infty} e^{-at}\int_0^t |e^{a\tau}h(\tau)|d\tau = 0.$$

Case b): $\lim_{t\to\infty}\int_0^t |e^{a\tau}h(\tau)|d\tau = \infty$.

By resorting to the famous L'Hôpital's rule, one first has

$$\begin{aligned}\lim_{t\to\infty}\int_0^t |e^{-a(t-\tau)}h(\tau)|d\tau\\ = \lim_{t\to\infty}\frac{\int_0^t |e^{a\tau}h(\tau)|d\tau}{e^{at}} = \lim_{t\to\infty}\frac{|e^{at}h(t)|}{ae^{at}}.\end{aligned}$$

Due to $\lim_{t\to\infty}h(t) = 0$, there are two continuously differentiable functions $h^+(t) \geq 0$ and $h^-(t) \leq 0$ satisfying $h^-(t) \leq h(t) \leq h^+(t)$ and $\lim_{t\to\infty}h^+(t) = \lim_{t\to\infty}h^-(t) = 0$. Furthermore, it can be concluded that

$$\begin{aligned}0 &\leq \lim_{t\to\infty}\frac{|e^{at}h(t)|}{ae^{at}}\\ &\leq \max\left\{-\lim_{t\to\infty}\frac{e^{at}h^-(t)}{ae^{at}}, \lim_{t\to\infty}\frac{e^{at}h^+(t)}{ae^{at}}\right\} = 0\end{aligned}$$

which implies $\lim_{t\to\infty}\int_0^t |e^{-a(t-\tau)}h(\tau)|d\tau = 0$.

Synthesizing both case a) and case b), one has that (21) is true, which completes the proof. ■

Lemma 4: Platooning control of the saturation-free vehicular system consisting of leader (2) and followers (1) can be achieved if, for any $i \in \{1, 2, \ldots, m\}$, one of the following conditions holds.

C1: The auxiliary error subsystem is stable

$$\begin{aligned}\dot{\bar{e}}_{vi}(t) = &(A + \lambda_i BK)\bar{e}_{vi}(t) + \lambda_i BK\bar{z}_i(t)\\ &- \lambda_i BK\bar{e}_{oi}(t) - \lambda_i BK(\bar{z}_0(t) + \bar{e}_{o0}(t))\end{aligned} \quad (22)$$

where $\bar{e}_{vi}(t)$, $\bar{z}_i(t)$ and $\bar{e}_{oi}(t)$ are the subvectors related to Jordan matrix J_i.

C2: The matrix $A + \lambda_i BK$ is Hurwitz,

where the inputs satisfy

$$\begin{aligned}\lim_{t\to\infty}\|\bar{e}_{o0}(t)\| = 0, \ \lim_{t\to\infty}\|\bar{z}_0(t)\| = 0\\ \lim_{t\to\infty}\|\bar{e}_{oi}(t)\| = 0, \ \lim_{t\to\infty}\|\bar{z}_i(t)\| = 0.\end{aligned}$$

Proof: According to the structure of Jordan matrix J, the saturation-free system (16) can be easily decomposed into m subsystems. Without loss of generality, its ith subsystem with state $\bar{e}_{vi}(t) = [\bar{e}_{vi1}^\top\ \bar{e}_{vi2}^\top \cdots \bar{e}_{vil}^\top]^\top$ corresponding Jordan block $J_i \in \mathbb{R}^{l\times l}$ can be further rewritten as follows:

$$\begin{aligned}\dot{\bar{e}}_{vis}(t) = &(A + \lambda_i BK)\bar{e}_{vis}(t) + \lambda_i BK\bar{z}_{is}(t)\\ &- \lambda_i BK\bar{e}_{ois}(t) - \lambda_i BK(\bar{z}_0(t)\\ &+ BK\bar{e}_{vi,s+1}(t) + BK\bar{z}_{i,s+1}(t)\\ &- BK\bar{e}_{oi,s+1}(t) - BK(\bar{z}_0(t) + \bar{e}_{o0}(t))\\ &+ \bar{e}_{o0}(t)), \qquad 1 \leq s \leq l-1\end{aligned} \quad (23a)$$

$$\begin{aligned}\dot{\bar{e}}_{vil}(t) = &(A + \lambda_i BK)\bar{e}_{vil}(t) + \lambda_i BK\bar{z}_{il}(t)\\ &- \lambda_i BK\bar{e}_{oil}(t) - \lambda_i BK(\bar{z}_0(t) + \bar{e}_{o0}(t))\end{aligned} \quad (23b)$$

where the structure of vectors $\bar{z}_i(t)$ and $\bar{e}_{oi}(t)$ is the same as $\bar{e}_{vi}(t)$.

According to condition C2, Lemma 3, as well as the solution of linear systems, one has the subsystem (23b) is stable, that is, $\lim_{t\to\infty}\|\bar{e}_{vil}(t)\| = 0$. In what follows, let us disclose the stability of subsystems (23a) via the well-known mathematical induction. To this end, assume that $\lim_{t\to\infty}\|\bar{e}_{vi,s+1}(t)\| = 0$ holds and let us disclose $\lim_{t\to\infty}\|\bar{e}_{vi,s}(t)\| = 0$.

It is not difficult to find that the solution of (23a) can be written as

$$\begin{aligned}\bar{e}_{vis}(t) = &\mathbf{e}^{(A+\lambda_i BK)t}\bar{e}_{vis}(0)\\ &+ \int_0^t \mathbf{e}^{(A+\lambda_i BK)(t-\tau)}BK\bar{e}_{vi,s+1}(\tau)d\tau\\ &+ \int_0^t \mathbf{e}^{(A+\lambda_i BK)(t-\tau)}\varphi_{is}(\tau)d\tau\end{aligned}$$

where

$$\begin{aligned}\varphi_{is}(t) = &\lambda_i BK\bar{z}_{is}(t) + BK\bar{z}_{i,s+1}(t)\\ &- \lambda_i BK\bar{e}_{ois}(t) - \lambda_i BK(\bar{z}_0(t) + \bar{e}_{o0}(t))\\ &- BK\bar{e}_{oi,s+1}(t) - BK(\bar{z}_0(t) + \bar{e}_{o0}(t)).\end{aligned}$$

Due to $\lim_{t\to\infty}\varphi_{is}(t) = 0$, applying the condition C2 and Lemma 3 again results in $\lim_{t\to\infty}\bar{e}_{vis}(t) = 0$. As such, according to mathematical induction, one has the ith subsystem of (16) is stable, that is, the platooning control of the saturation-free vehicular system is achieved.

On the other hand, according to the relationship between the subsystem (23a) and (23b) and the auxiliary error subsystem (22), one can easily obtain that the platooning control can be achieved if the condition C1 is true, and the proof is completed. ■

C. Stability Analysis and Controller Gain Design

It should be indicated that the challenge from digraphs is the specific structure Jordan matrix J in platooning error dynamics (16). Benefitting from Lemma 4, such a challenge can be effectively handled by resorting to an auxiliary system consisting of a set of subsystems matched with the last row of each Jordan block. By doing so, one first stack the eigenvalues of $\mathcal{L} + \mathcal{D}_0$ into an $N \times N$ diagonal matrix $\Lambda = \text{diag}\{\lambda_1, \ldots, \lambda_1, \ldots, \lambda_2, \ldots, \lambda_2, \ldots, \lambda_m, \ldots, \lambda_m\}$, where the multiplicity of each eigenvalue equals to the dimension of its corresponding Jordan matrix. Then, define a composite vector $w(t) = -\mathbf{1}_N \otimes (\bar{z}_0(t) + \bar{e}_{o0}(t))$ and an augmented vector $\zeta(t) = [\bar{e}_v^\top(t)\ \bar{e}_o^\top(t)\ \bar{r}^\top(t)]^\top$. Considering the relationship among (5), (16), and (22) in Lemma 4, one can obtain the following *auxiliary* system:

$$\dot{\zeta}(t) = \mathcal{A}\zeta(t) + \mathcal{E}_1 z(t) + \mathcal{F}_1\bar{\Psi}(\tilde{u}(t)) + \mathcal{F}_2 w(t) \quad (24)$$

where

$$\mathcal{A} = \begin{bmatrix} A_{11} & A_{12} & 0\\ 0 & A_{22} & -I_N \otimes L_I\\ 0 & I_N \otimes C & -\phi I_{Nq}\end{bmatrix}$$

$$\begin{aligned}&A_{11} = I_N \otimes A + \Lambda \otimes BK,\ A_{12} = -\Lambda \otimes BK\\ &A_{22} = I_N \otimes A - I_N \otimes L_P C,\ \mathcal{E}_1 = \begin{bmatrix}A_{12}^\top & 0 & 0\end{bmatrix}^\top\\ &\mathcal{F}_1 = \begin{bmatrix}-I_N \otimes B^\top & 0 & 0\end{bmatrix}^\top,\ \mathcal{F}_2 = \begin{bmatrix}(\Lambda \otimes BK)^\top & 0 & 0\end{bmatrix}^\top.\end{aligned}$$

Now, the platooning control problem of the addressed vehicular system (1) with PIO (4), encryptor (7), and decryptor (9) is transformed into the stability analysis issue of the above *auxiliary* system. The corresponding result is stated in the following theorem.

Theorem 2: Consider a vehicular platoon consisting of (1) with PIO (4), encryptor (7), and decryptor (9). Furthermore, observer gains L_I and L_P of PIO (4) are designed via the condition in Theorem 1. The platooning requirement with the specified spacing reference is guaranteed if there exist a positive definite matrix P, a matrix $\tilde{K}$, and two positive scalars $\iota \in (0,1)$ and $\epsilon_1 > 0$ such that

$$\Xi_2(\lambda_i) = \begin{bmatrix} \tilde{\Xi}_{11}+\tilde{\Xi}_{11}^\top & \tilde{\Xi}_{12} & \tilde{\Xi}_{13} & \tilde{\Xi}_{14} \\ * & \tilde{\Xi}_{22} & -\tilde{\Xi}_{13} & \mathbf{0} \\ * & * & \tilde{\Xi}_{33} & \mathbf{0} \\ * & * & * & -\epsilon_1 I \end{bmatrix} < 0 \quad (25)$$

for $i=1$ and $i=N$, where

$$\begin{aligned} &\tilde{\Xi}_{11} = A\tilde{P} + \lambda_i B\tilde{K},\ \tilde{\Xi}_{12} = \lambda_i B\tilde{K},\ \tilde{\Xi}_{13} = \tilde{K}^\top \\ &\tilde{\Xi}_{14} = \epsilon_1 B,\ \tilde{\Xi}_{22} = \lambda_{\max}(\Xi_1)\big(2\tilde{P} - I_3\big) \\ &\tilde{\Xi}_{33} = -\epsilon_1\iota(\lambda_N+1)\lambda_{\max}(\Gamma)\lambda_{\min}^{-1}(\Gamma)I_q \end{aligned}$$

and, meanwhile, parameters are selected as

$$\begin{aligned} &\gamma \in \left(\mathbf{e}^{\frac{\vartheta}{2\lambda_{\max}(Q)}}, 1\right),\ \eta \in (0,1),\ a_0 = 2\sqrt{2}(1+\eta) \\ &\rho_0 > 1,\ \rho_1 = \|\Gamma \otimes B\|,\ \rho_2 = \frac{(\lambda_N+1)\|K\|}{\sqrt{\|\mathcal{P}\|}} \\ &\rho_3 = (\lambda_N+1)\|K\|,\ K = \tilde{K}\tilde{P}^{-1},\ \vartheta = \lambda_{\max}(\Xi_1) \\ &\epsilon_2 = \max\{|\lambda(\Xi_2(\lambda_1))|, |\lambda(\Xi_2(\lambda_N))|\} \\ &g_1 \geq \ln(\beta)\ln^{-1}(\alpha),\ \beta \in \left((1+2\eta)^{-1}, 1\right) \\ &T \leq \min\left\{\frac{\ln(\rho_0)}{\|A\|}, \frac{\epsilon_2}{a_0\rho_0\rho_1\rho_2\|E_4\|\sqrt{\|P\|} + \epsilon_2\rho_0\rho_1\rho_3}\right\}. \end{aligned}$$

Proof: Select the Lyapunov function as

$$V(t) = \zeta^\top(t)\mathcal{P}\zeta(t) \quad (26)$$

where $\mathcal{P} = \mathrm{diag}\{I_N \otimes P, I_N \otimes Q_1, I_N \otimes Q_2\}$ with Q_1 and Q_2 acquired from Theorem 1. Differentiating (26) along dynamics (24) leads to

$$\begin{aligned} \dot{V}(t) &= 2\zeta^\top(t)\,\mathcal{P}\big(\mathcal{A}\zeta(t) + \mathcal{E}_1 z(t) + \mathcal{F}_1\bar{\Psi}(\tilde{u}(t)) + \mathcal{F}_2 w(t)\big) \\ &= 2\bar{e}_v^\top(t)(I_N\otimes P)A_{11}\bar{e}_v(t) + 2\bar{e}_v^\top(t)(I_N\otimes P)A_{12}\bar{e}_v(t) \\ &\quad + 2\bar{e}_o^\top(t)(I_N\otimes Q_1)A_{22}\bar{e}_o(t) - 2\bar{e}_o^\top(t)(I_N\otimes Q_1L_I)\bar{r}(t) \\ &\quad + 2\bar{r}^\top(t)(I_N\otimes Q_2C)\bar{e}_o(t) - 2\bar{r}^\top(t)(I_N\otimes Q_2)\bar{r}(t) \\ &\quad + 2\zeta^\top(t)\,\mathcal{P}\mathcal{E}_1 z(t) + \zeta^\top(t)\,\mathcal{P}\mathcal{F}_1\bar{\Psi}(\tilde{u}(t)) + \zeta^\top(t)\,\mathcal{P}\mathcal{F}_2 w(t). \end{aligned}$$

Considering

$$\begin{aligned} &2\bar{e}_o^\top(t)(I_N\otimes Q_1)A_{22}\bar{e}_o(t) - 2\bar{e}_o^\top(t)(I_N\otimes Q_1L_I)\bar{r}(t) \\ &\quad + 2\bar{r}^\top(t)(I_N\otimes Q_2C)\bar{e}_o(t) - 2\bar{r}^\top(t)(I_N\otimes Q_2)\bar{r}(t) \\ &= \big[\bar{e}_o^\top(t) \quad \bar{r}^\top(t)\big](I_N\otimes\Xi_1)\big[\bar{e}_o^\top(t) \quad \bar{r}^\top(t)\big]^\top \end{aligned}$$

with Ξ_1 from Theorem 1, one has

$$\begin{aligned} \dot{V}(t) &\leq 2\bar{e}_v^\top(t)(I_N\otimes P_1)A_{11}\bar{e}_v(t) + 2\bar{e}_v^\top(t)(I_N\otimes P_1)A_{12}\bar{e}_v(t) \\ &\quad + \lambda_{\max}(\Xi_1)\Big(\bar{e}_o^\top(t)\bar{e}_o(t) + \bar{r}^\top(t)\bar{r}\Big) + 2\zeta^\top(t)\,\mathcal{P}\mathcal{E}_1 z(t) \\ &\quad + \zeta^\top(t)\,\mathcal{P}\mathcal{F}_1\bar{\Psi}(\tilde{u}(t)) + \zeta^\top(t)\,\mathcal{P}\mathcal{F}_2 w(t) \\ &\leq \zeta^\top\Big(\bar{\mathcal{A}} + \bar{\mathcal{A}}^\top\Big)\zeta(t) + 2\zeta^\top(t)\mathcal{P}\mathcal{E}_1\bar{z}(t) \\ &\quad + 2\zeta^\top(t)\mathcal{P}\mathcal{F}_2 w(t) + 2\zeta^\top\mathcal{P}\mathcal{F}_1\bar{\Psi}(\tilde{u}(t)) \end{aligned}$$

where

$$\bar{\mathcal{A}} = \begin{bmatrix} \bar{A}_{11} & \bar{A}_{12} & \mathbf{0} \\ \mathbf{0} & \frac{\lambda_{\max}(\Xi_1)}{2}I_3 & \mathbf{0} \\ \mathbf{0} & \mathbf{0} & \frac{\lambda_{\max}(\Xi_1)}{2}I_q \end{bmatrix}$$

$$\bar{A}_{11} = I_N\otimes PA + \Lambda\otimes PBK,\ \bar{A}_{12} = -\Lambda\otimes PBK.$$

Due to the fact that

$$\begin{aligned} &2\zeta^\top\mathcal{P}\mathcal{F}_1\Psi(\tilde{u}(t)) \\ &\quad \leq \epsilon_1\zeta^\top(t)\mathcal{P}\mathcal{F}_1\mathcal{F}_1^\top\mathcal{P}\zeta(t) + \epsilon_1^{-1}\bar{\Psi}^\top(\tilde{u}(t))\bar{\Psi}(\tilde{u}(t)) \end{aligned}$$

recalling Lemma 1 and (13), one has

$$\begin{aligned} &\bar{\Psi}^T(\tilde{u}(t))\bar{\Psi}(\tilde{u}(t)) \\ &\quad \leq \iota\tilde{u}^\top(t)\Big(\Gamma^\top\Gamma\otimes I_3\Big)\tilde{u}(t) \\ &\quad \leq \epsilon_3^2(\zeta^T(t)\bar{A}_{14}^\top\bar{A}_{14}\zeta(t) \\ &\qquad + 2\zeta^T(t)\bar{A}_{14}^\top A_{14}\bar{z}(t) + 2\zeta^T(t)\bar{A}_{14}^\top A_{14}w(t) \\ &\qquad + \bar{z}^T(t)A_{14}^\top A_{14}\bar{z}(t) + 2w^T(t)A_{14}^\top A_{14}\bar{z}(t) \\ &\qquad + w^T(t)A_{14}^\top A_{14}w(t) \end{aligned}$$

where

$$\begin{aligned} &\bar{A}_{14} = [A_{14}, -A_{14}, \mathbf{0}]^\top,\ A_{14} = I_N\otimes K. \\ &\epsilon_3 = \sqrt{\iota}(\lambda_N+1)\lambda_{\max}(\Gamma)/\lambda_{\min}(\Gamma). \end{aligned}$$

Taking the above inequality into account, one has

$$\begin{aligned} \dot{V}(t) &\leq \zeta^\top\Big(\bar{\mathcal{A}} + \bar{\mathcal{A}}^\top + \mathcal{P}\mathcal{F}_1\mathcal{F}_1^\top\mathcal{P} + \epsilon_3^2\bar{A}_{14}^\top\bar{A}_{14}\Big)\zeta(t) \\ &\quad + 2\zeta^\top(t)\mathcal{P}\mathcal{E}_1\bar{z}(t) + 2\zeta^\top(t)\mathcal{P}w(t) \\ &\quad + 2\epsilon_3^2\zeta^\top(t)\bar{A}_{14}^\top A_{14}\bar{z}(t) + \epsilon_3^2\bar{z}^\top(t)A_{14}^\top A_{14}\bar{z}(t) \\ &\quad + 2\epsilon_3^2 w^\top(t)A_{14}^\top A_{14}\bar{z}(t) + 2\epsilon_3^2\zeta^\top(t)\bar{A}_{14}^\top A_{14}w(t) \\ &\quad + \epsilon_3^2 w^\top(t)A_{14}^\top A_{14}w(t). \end{aligned} \quad (27)$$

To proceed with, let us first assume that

$$\bar{\mathcal{A}} + \bar{\mathcal{A}}^\top + \mathcal{P}\mathcal{F}_1\mathcal{F}_1^\top\mathcal{P} + \epsilon_3^2\bar{A}_{14}^\top\bar{A}_{14} < 0 \quad (28)$$

holds. Such an assumption can be guaranteed by (25) and will be verified in the later analysis. Then, there exists a positive constant ϵ_2 such that

$$\begin{aligned} \dot{V}(t) &\leq -\epsilon_2\zeta^\top(t)\zeta(t) + 2\zeta^\top(t)\mathcal{E}_2\bar{z}(t) \\ &\quad + 2\zeta^\top(t)\mathcal{E}_3 w(t) + \epsilon_3^2\bar{z}^\top(t)A_{14}^\top A_{14}\bar{z}(t) \\ &\quad + 2\epsilon_3^2 w^\top(t)A_{14}^\top A_{14}\bar{z}(t) \\ &\quad + \epsilon_3^2 w^\top(t)A_{14}^\top A_{14}w(t) \end{aligned} \quad (29)$$

where $\mathcal{E}_2 = \mathcal{P}\mathcal{E}_1 + \epsilon_3^2\bar{A}_{14}^\top A_{14}$ and $\mathcal{E}_3 = \mathcal{P}\mathcal{F}_2 + \epsilon_3^2\bar{A}_{14}^\top A_{14}$.

For the cross terms in (29), one has

$$\begin{aligned} &2\zeta^\top(t)\mathcal{E}_2\bar{z}(t) \\ &\quad \leq \frac{4(1+\eta)}{\epsilon_2}\bar{z}(t)\mathcal{E}_2^\top\mathcal{E}_2\bar{z}(t) + \frac{\epsilon_2}{4(1+\eta)}\zeta^\top(t)\zeta(t) \end{aligned} \quad (30)$$

$$\begin{aligned} &2\zeta^\top(t)\mathcal{E}_3 w(t) \\ &\quad \leq \frac{4(1+\eta)}{\epsilon_2}w^\top(t)\mathcal{E}_3^\top\mathcal{E}_3 w(t) + \frac{\epsilon_2}{4(1+\eta)}\zeta^\top(t)\zeta(t) \end{aligned} \quad (31)$$

$$\begin{aligned}&2\epsilon_3 w^\top(t)A_{14}^\top A_{14}\bar{z}(t)\\&\quad\le \frac{\epsilon_2\epsilon_3^2}{4(1+\eta)}w^\top(t)A_{14}^\top A_{14}w(t)\\&\qquad+\frac{4(1+\eta)\epsilon_3^2}{\epsilon_2}\bar{z}^\top(t)A_{14}^\top A_{14}\bar{z}(t)\end{aligned}\tag{32}$$

where η is a positive constant. In what follows, substituting (30)–(32) into (29) yields

$$\begin{aligned}\dot{V}(t)&\le -\epsilon_2\frac{1+\eta}{1+\eta}\zeta^\top(t)\zeta(t)+\frac{\epsilon_2}{2(1+\eta)}\zeta^\top(t)\zeta(t)\\&\quad+\frac{4(1+\eta)}{\epsilon_2}\bar{z}\top(t)\mathcal{E}_4^\top\mathcal{E}_4\bar{z}(t)\\&\quad+\frac{4(1+\eta)}{\epsilon_2}w^\top(t)\mathcal{E}_5^\top\mathcal{E}_5 w(t)\\&\le -\frac{\epsilon_2\eta}{1+\eta}\|\zeta(t)\|^2-\frac{1}{2\epsilon_2(1+\eta)}\Big(\epsilon_2^2\|\zeta(t)\|^2\\&\quad-8(1+\eta)^2\big(\|\mathcal{E}_4\|^2\|z(t)\|^2-\|\mathcal{E}_5\|^2\|w(t)\|^2\big)\Big)\end{aligned}\tag{33}$$

where $\mathcal{E}_4=\left[\mathcal{E}_2^\top \ \ \epsilon_3 A_{14}^\top\right]^\top$ and $\mathcal{E}_5=\left[\mathcal{E}_3^\top \ \ \epsilon_3 A_{14}^\top\right]^\top$.

Up to now, it is obvious that the first part $-\epsilon_2\eta(1+\eta)^{-1}\zeta^\top(t)\zeta(t)$ in $\dot{V}(t)$ is negative. However, it is hard to determine whether the remaining part is negative or not because there exist jump phenomena in $\bar{z}(t)$ as the communication between vehicles is not continuous.

As such, to deal with this challenge, one needs to reveal that the upper bound of $V(t)$ over a given time interval is nonincreasing and will decrease to zero as time goes infinity. Inspired by [34], the following proof will be laid out in three parts.

1) Upper Bound of $\bar{z}(t)$: It follows from (4) and (7) that:

$$\begin{cases}\dot{\bar{z}}(t)=(I_N\otimes A)\bar{z}(t)\\ -(\Gamma\otimes B)\tilde{u}(t)-(I_N\otimes L_P C)e_o(t)\\ \dot{\bar{z}}_0(t)=(I_N\otimes A)\bar{z}_0(t)-(I_N\otimes L_P C)e_{o0}(t).\end{cases}$$

Solving these differential equations in $t\in(kg_1T,(kg_1+1)T)$, one has

$$\begin{aligned}\bar{z}(t)&=\Big(I_N\otimes e^{A(t-kT)}\Big)\bar{z}(kT)\\&\quad-\int_{kT}^t\Big(I_N\otimes e^{A(t-kT)}\Big)(\Gamma\otimes B)\tilde{u}(\tau)d\tau\\&\quad-\int_{kT}^t\Big(I_N\otimes e^{A(t-kT)}\Big)(I_N\otimes L_P C)\bar{e}_o(\tau)d\tau\end{aligned}\tag{34}$$

and

$$\begin{aligned}\bar{z}_0(t)&=\Big(I_N\otimes e^{A(t-kT)}\Big)\bar{z}_0(kT)\\&\quad-\int_{kT}^t\Big(I_N\otimes e^{A(t-kT)}\Big)(I_N\otimes L_P C)\bar{e}_{o0}(\tau)d\tau.\end{aligned}\tag{35}$$

For the notational simplicity, denote

$$\rho_4=\|L_P C\|,\ \ \rho_5=\sqrt{\frac{V_o(0)}{\lambda_{\min}(Q)}}\frac{\|\Gamma\|}{\ln(\gamma)b_0\hbar\sqrt{3N}\mathbf{e}^{\|\mathcal{A}_c\|T}}.$$

Because of $\gamma\in(\mathbf{e}^{-(\vartheta/[2\lambda_{\max}(Q)}, 1)$, condition (20) and Lemma 2, the upper bound of the last term in (35) is

$$\begin{aligned}&\int_{kT}^t\Big\|\mathbf{e}^{A(t-kT)}\Big\|\|L_P C\|\|\bar{e}_{o0}(\tau)\|d\tau\\&\le\int_{kT}^{(k+1)T}\rho_4\mathbf{e}^{\|A\|T}\sqrt{\frac{V_o(0)}{\lambda_{\min}(Q)}}\|\Gamma\|\gamma^{kT}d\tau\\&=\rho_4\mathbf{e}^{\|A\|T}\sqrt{\frac{V_o(0)}{\lambda_{\min}(Q)}}\frac{\|\Gamma\|}{\ln\gamma}T\gamma^{kT}\\&=\rho_4\mathbf{e}^{\|A\|T}\sqrt{\frac{V_o(0)}{\lambda_{\min}(Q)}}\frac{\|\Gamma\|}{\ln\gamma}\frac{Tb(kT)}{b_0\hbar\sqrt{3N}\mathbf{e}^{\|\mathcal{A}_c\|T}}\\&=\rho_4\rho_5\mathbf{e}^{\|A\|T}Tb(kT).\end{aligned}\tag{36}$$

If the selected sampling period T satisfies $T\le([\ln(\rho_0)]/[\|A\|])$, (i.e., $\rho_0>\mathbf{e}^{\|A\|T}$), one has

$$\int_{kT}^t\Big(I_N\otimes e^{A(t-kT)}L_P C\Big)\bar{e}_{o0}(\tau)d\tau\le\rho_0\rho_4\rho_5 Tb(kT).\tag{37}$$

Similarly, the upper bound of the last term in (34) is

$$\int_{kT}^t\Big(I_N\otimes e^{A(t-kT)}L_P C\Big)\bar{e}_o(\tau)d\tau\le\rho_0\rho_4\rho_5 T\sqrt{N}b(kT).\tag{38}$$

In what follows, denote:

$$\begin{aligned}v_{\sup,k}&=\sup_{t\in[kT,(1g_1+1)T)}\sqrt{V(t)}\\ \bar{z}_{\sup,k}&=\sup_{t\in[kT,(kg_1+1)T)}\|\bar{z}(t)\|\\ \bar{z}_{\sup,0k}&=\sup_{t\in[kT,(kg_1+1)T)}\|\bar{z}_0(t)\|.\end{aligned}$$

Combining with (13), one has the upper bound of the second term in (34) as

$$\begin{aligned}&\int_{kT}^t\Big(I_N\otimes e^{A(t-kT)}\Big)(\Gamma\otimes B)\tilde{u}(\tau)d\tau\\&\quad\le\int_{kT}^t\rho_0\|J\otimes BK\|(\|\bar{e}_v(t)\|+\|\bar{z}(t)\|+\|\bar{e}_o(t)\|\\&\qquad+\sqrt{N}\|\bar{z}_0(t)\|+\sqrt{N}\|\bar{e}_{o0}(t)\|\Big).\end{aligned}$$

Then, considering the relationship

$$\int_{kT}^t\|e_v(\tau)\|d\tau\le\int_{kT}^t\frac{\sqrt{V(\tau)}}{\sqrt{\|\mathcal{P}\|}}d\tau\le\frac{1}{\sqrt{\|\mathcal{P}\|}}Tv_{kT}$$

and the fact $\|J\|\le\lambda_N+1$, one has

$$\begin{aligned}&\int_{kT}^t\Big(I_N\otimes e^{A(t-kT)}\Big)(\Gamma\otimes B)\tilde{u}(\tau)d\tau\\&\quad\le\rho_0\rho_1\rho_2 Tv_{\sup,k}+\rho_0\rho_1\rho_3 T\bar{z}_{\sup,k}\\&\qquad+2\rho_0\rho_1\rho_3\rho_5 T\sqrt{N}b(kT)\\&\qquad+\rho_0\rho_1\rho_3 T\sqrt{N}\bar{z}_{\sup,0k}.\end{aligned}\tag{39}$$

Summarizing the inequalities above yields

$$\begin{aligned}\|\bar{z}(t)\|&\le\rho_0\|\bar{z}(kT)\|+\rho_0\rho_1\rho_2 Tv_{\sup,k}\\&\quad+\rho_0\rho_1\rho_3 T\bar{z}_{\sup,k}+2\rho_0\rho_1\rho_3\rho_5 T\sqrt{N}b(kT)\\&\quad+\rho_0\rho_4\rho_5 T\sqrt{N}b(kT)+\rho_0\rho_1\rho_3 T\sqrt{N}\bar{z}_{\sup,0k}.\end{aligned}\tag{40}$$

Following the same steps, one can also obtain:

$$\|z_0(t)\|\le\rho_0\|z_0(kT)\|+\rho_0\rho_4\rho_5 Tb(kT)$$

which indicates

$$z_{\sup,0k}\le\left(\frac{\rho_0}{\mathbf{e}^{\|\mathcal{A}_c\|T}}+\rho_0\rho_4\rho_5\right)b(kT).\tag{41}$$

Finally, denoting

$$a_1 = 1 - \rho_0\rho_1\rho_3 T,\ a_2 = \frac{\rho_0\rho_1\rho_2 T}{a_1},\ a_3 = \rho_0/\mathbf{e}^{\|\mathcal{A}_c\|T}$$
$$a_4 = \frac{a_3 + \rho_0\sqrt{N}\big(\rho_5 T(2\rho_1\rho_3 + \rho_4) + \rho_1\rho_3(a_3 + \rho_0\rho_4\rho_5 T)\big)}{a_1}$$

and recalling Lemma 2, one has

$$z_{\sup,k} \le a_4 b(kT) + a_2 v_{\sup,k}. \tag{42}$$

Taking (40)–(42) into consideration, one arrives at that $\bar{z}(t)$ is bounded.

2) Nonincreasing Function $V(t)$: Due to the fact $\lim_{t\to\infty} b(t) = 0$, it follows from (38) and (41) that $\lim_{t\to\infty} e_{o0}(t) = 0$ and $\lim_{t\to\infty} z_0(t) = 0$ and, hence, their combination $\lim_{t\to\infty}\|w(t)\| = 0$.

In what follows, substituting (42) into (33) generates:

$$\begin{aligned}\dot{V}(t) \le &-\frac{1}{2\epsilon_2(1+\eta)}\Big(\epsilon_2^2\|\mathcal{P}\|^{-1}\Big(V(t) - v_{\sup,k}^2\Big)\\ &+ f_1\big(v_{\sup,k}\big)\Big) - \frac{\epsilon_2\eta}{1+\eta}\zeta^\top(t)\zeta(t)\end{aligned} \tag{43}$$

where

$$\begin{aligned}f_2\big(v_{\sup,k}\big) &= \Big(\epsilon_2^2\|\mathcal{P}\|^{-1} - a_0^2 a_2^2\|\mathcal{E}_4\|^2\Big)v_{\sup,k}^2 - a_0^2 a_4^2\\ &\quad\times \|\mathcal{E}_4\|^2 b^2(kT) - 2a_0^2\|\mathcal{E}_4\|^2 a_2 a_4 b(kT) v_{\sup,k}\\ f_1\big(v_{\sup,k}\big) &= f_2\big(v_{\sup,k}\big) - 8(1+\eta)^2\|\mathcal{E}_5\|\|w(t)\|^2.\end{aligned}$$

It can be easily observed the positiveness or negativeness of $\dot{V}(t)$ is determined by $\epsilon_2^2/\|P\|(V(t) - v_{\sup,k}^2) + f_1(v_{\sup,k})$.

Recalling that the selected T satisfies

$$T < \epsilon_2\big(a_0\|\mathcal{E}_4\|\sqrt{\|\mathcal{P}\|}\rho_0\rho_1\rho_2 + \epsilon_2\rho_0\rho_1\rho_3\big)^{-1}$$

one has $\epsilon_2^2\|\mathcal{P}\|^{-1} - a_0^2 a_2^2\|\mathcal{E}_4\|^2 > 0$. In light of the discriminant for polynomials, it is not difficult to conclude that $f_1(v_{kT}) = 0$ has two roots $r_1(kT)$ and $r_2(kT)$ satisfying $r_1(kT) < 0 < r_2(kT)$. Furthermore, one has $f_1(v) > 0$ if $v > r_2(kT)$.

Now, we are the position to disclose that $V(t)$ is nonincreasing for any $t \in [kg_1 T, (k+1)g_1 T)$ $(k \in \mathbb{N})$, which is divided into two cases.

Case a): $V(kg_1T) < r_2^2(kg_1T)$.

If the upper bound is achieved at the left end point, that is, $v_{\sup,kg_1}^2 = V(kg_1T)$, one has $V(t) < V(kg_1T) < r_2^2(kg_1T)$ from the definition of $v_{\sup,kg_1}$. On the contrary, if there exists an instant $t' \in (kg_1T, (kg_1+1)T)$ such that $V(t') = v_{\sup,kg_1}^2 > r_2^2(kg_1T)$, one has $f_1(v_{\sup,kg_1}) > 0$. Furthermore, it follows from (43) that $\dot{V}(t') < 0$. Since $\dot{V}(t)$ is a locally continuous function, there exists $t'' \in [kg_1T, t')$ such that $V(t'') > V(t')$, which contradicts the definition of $v_{\sup,kg_1}$. As such, the conclusion $V(t) < V(kg_1T) < r_2^2(kg_1T)$ holds for any $t \in [kg_1T, (kg_1+1)T)$.

Case b): $V(kg_1T) \ge r_2^2(kg_1T)$.

In this case, the conclusion $V(t) \le V(kg_1T)$ for $t \in [kg_1T, (kg_1+1)T)$ will be revealed via contradiction. Since $V(kg_1T) \ge r_2^2(kg_1T)$, one first has $f_1(v_{\sup,kg_1}) > 0$. Then, suppose there exists an instant $t' \in [kg_1T, (kg_1+1)T)$ such that $V(t') = v_{\sup,kg_1}^2 > V(kg_1T)$. Similar to case a), one has $\dot{V}(t') < 0$ due to (43) combined with the fact $f_1(v_{\sup,kg_1}) > 0$. Furthermore, there exists an instant $t'' \in [kg_1T, t')$ such that $V(t'') > V(t')$, which contradicts the definition of $v_{\sup,kg_1}$. As such, the conclusion $V(t) \le V(kg_1T)$ holds for any $t \in [kg_1T, (kg_1+1)T)$.

Noting that $b(t) \equiv b(kg_1T)$ and $e_{o,kg_1T} \ge e_o(t)$ for any $t \in [kg_1T, (k+1)g_1T)$, it is easy to extend the results above on the interval $[kg_1T, (kg_1+1)T)$ to the interval $t \in [kg_1T, (k+1)g_1T)$. Finally, synthesizing case a) and case b), one has that $V(t)$ is nonincreasing. In what follows, let us disclose the convergence of function $V(t)$.

3) Convergence of Function $V(t)$: Recalling case b) above, one can simplify (43) to

$$\dot{V}(t) \le -\aleph_1 V(t) + \aleph_2 v_{kT}^2,\quad t \in \big[kg_1T, (kg_1+1)T\big) \tag{44}$$

where $\aleph_1 = ([\epsilon_2(1+2\eta)]/[2\|\mathcal{P}\|(1+\eta)])$ and $\aleph_2 = (\epsilon_2/[2(1+\eta)\|\mathcal{P}\|])$. Solving such a differential equation yields

$$\begin{aligned}V(t) \le e^{-\aleph_1 T}\big(&V(kg_1T)\\ &- (1+2\eta)^{-1}v_{kg_1T}^2\big) + (1+2\eta)^{-1}v_{kg_1T}^2\end{aligned}$$

for $t \in [kg_1T, (kg_1+1)T]$. Then, considering the fact $v_{\sup,kg_1}^2 = V(kg_1T)$, one has

$$V((kg_1+1)T) \le \alpha V(kg_1T)$$

which iteratively results in

$$V((k+1)g_1T) \le \alpha^{g_1} V(kg_1T)$$

where $\alpha = e^{-\aleph_1 T}(1 - (1/1+2\eta)) + (1/1+2\eta)$. It is not difficult to verify $\alpha^{g_1} \in [(1/1+2\eta), 1)$. Furthermore, selecting $g_1 \ge (\ln(\beta)/\ln(\alpha))$ with $\beta \in ([1/1+2\eta], 1)$, one has

$$V((k+1)g_1T) \le \beta V(kg_1T). \tag{45}$$

Summarizing (45) and case a), one can obtain the upper bound

$$\begin{aligned}V(g_1T) &\le \max\Big\{r_3^2(0), \beta V(0)\Big\}\\ V(2g_1T) &\le \max\Big\{r_3^2(g_1T), \beta V(g_1T)\Big\}\\ &= \max\Big\{\gamma^2 r_3^2(0), \beta r_3^2(0), \beta^2 V(0)\Big\}.\end{aligned}$$

By iterative calculation, it can be obtained that

$$V(kg_1T) \le \max_{i\in\mathbb{N}^+}\Big\{\gamma^{2i}\beta^{k-1-i} r_3^2(0), \beta^k V(0)\Big\}.$$

Due to $\lim_{k\to\infty}\beta^k$ and $\lim_{k\to\infty}\gamma^{2i}\beta^{k-1-i} = 0$, one can conclude that $\lim_{k\to\infty} V(kg_1T) = 0$, which means $\lim_{t\to\infty}\zeta(t) = 0$. That is to say, the desired platooning requirement is achieved.

Finally, let us discuss condition (28). First, considering that $\bar{\mathcal{A}} + \bar{\mathcal{A}}^\top$ is a block matrix and Ξ_1 is negative definite, and applying the Schur complement, (28) is equivalent to

$$\begin{bmatrix}\tilde{A}_{11} + \tilde{A}_{11}^\top & \tilde{A}_{12} & \tilde{A}_{14} & \epsilon_1\tilde{A}_{15}\\ * & \tilde{A}_{22} & -\tilde{A}_{14} & \mathbf{0}\\ * & * & \tilde{A}_{44} & \mathbf{0}\\ * & * & * & -\epsilon_1\end{bmatrix} < 0 \tag{46}$$

for any λ_i $(i = 1, 2, \ldots, N)$, where

$$\tilde{A}_{11} = PA + \lambda_i PBK,\ \tilde{A}_{12} = \lambda_i PBK,\ \tilde{A}_{14} = K^\top$$

$$\tilde{A}_{15} = -PB,\ \tilde{A}_{22} = \lambda_{\max}(\Xi_1)I_3$$
$$\tilde{A}_{44} = -\epsilon_1\iota(\lambda_i + 1)\lambda_{\max}(\Gamma)/\lambda_{\min}(\Gamma)I_q.$$

Pre- and post-multiplying (46) by $\text{diag}\{P^{-1}, P^{-1}, I_p, 1\}$, one has that (28) is true if $\Xi_2(\lambda_i) < 0$ for any eigenvalues. On the other hand, there exists a constant $\theta_i \in [0, 1]$ $(i = 1, 2, \ldots, N)$ satisfying

$$\lambda_i = \theta_i\lambda_1 + (1 - \theta_i)\lambda_N. \quad (47)$$

As such, (28) is true only when both $\Xi_2(\lambda_1) < 0$ and $\Xi_2(\lambda_N) < 0$ hold, and the proof is now completed. ■

Remark 5: It should be pointed out that an executable condition only dependent of the maximum and minimum eigenvalues is derived in Theorem 2 via an auxiliary system. In this theorem, the effect from the digraph is reflected by the transformation matrix Γ and the suitable range is discovered for parameters in the dynamic private key $g(t)$.

Finally, it is worth noting that the key $g(t)$ tends to zero due mainly to $\gamma < 1$. If $\Delta_i(t)$ diverges to be infinity, then an infinite data rate is needed for information transmission, which is not applicable in practical engineering. As such, one has to further determine this parameter to avoid the phenomenon that $\Delta_i(t)$ is unbounded.

Theorem 3: The size of transmitted data is bounded if $\beta \leq \gamma^2$, that is, $\|\Delta_i(kT)\| < \infty$.

Proof: First, at time instant $(k+1)T \in [kg_1T, (k+1)g_1T)$ $(k \in \mathbb{N})$, one obtains

$$\|\Delta_i(t)\| \leq \left\| \frac{\mathbf{e}^{\mathcal{A}_c(t-kT)}\chi_i(kT) - \mathbf{e}^{\mathcal{A}_cT}\xi_i(kT)}{g((k+1)T)} \right\| + \left\| \frac{\int_{kT}^{t} \mathbf{e}^{\mathcal{A}_c(t-kT)}(I_N \otimes B)u(\tau)d\tau}{g((k+1)T)} \right\| + \left\| \frac{\int_{kT}^{t} \mathbf{e}^{\mathcal{A}_c(t-kT)}Le_o(\tau)d\tau}{g((k+1)T)} \right\| \quad (48)$$

for $\forall i \in \mathcal{V}$, where $L = \left[C^\top L_P^\top\ C^\top\right]^\top$. It follows from (7) that the upper bound of the first term can be calculated as:

$$\left\| \frac{\mathbf{e}^{\mathcal{A}_c(t-kT)}\tilde{x}_i(kT) - \mathbf{e}^{\mathcal{A}_cT}\xi_i(kT)}{g((k+1)T)} \right\| \leq \frac{\hbar\sqrt{3+q}\mathbf{e}^{\|\mathcal{A}_c\|T}}{\gamma} \triangleq c_1.$$

For the second term, one has

$$\left\| \frac{\int_{kT}^{t} \mathbf{e}^{\mathcal{A}_c(t-kT)}(I_N \otimes B)\tilde{u}(\tau)d\tau}{g((k+1)T)} \right\| \leq \frac{\mathbf{e}^{\|\mathcal{A}_c\|T}\|B\|}{g((k+1)T)} \int_{kT}^{t} \|u(\tau)\|d\tau. \quad (49)$$

With the help of (39) and (42), it follows:

$$\int_{kT}^{t} \|u(\tau)\|d\tau \leq \rho_2Tv_{\text{sup},k} + \rho_3T\bar{z}_{\text{sup},k} + 2\sqrt{N}\rho_3\rho_5Tb(kT) + \sqrt{N}\rho_3T\bar{z}_{\text{sup},0k}.$$

When the selected β satisfies $\beta \leq \gamma^2$, one has

$$\lim_{k\to\infty} \frac{v_{\text{sup},k}}{g((k+1)T)} \leq \lim_{k\to\infty} \max\left\{\gamma^{2k-2}r_3^2(0), \beta^kV(0)\right\} = 0.$$

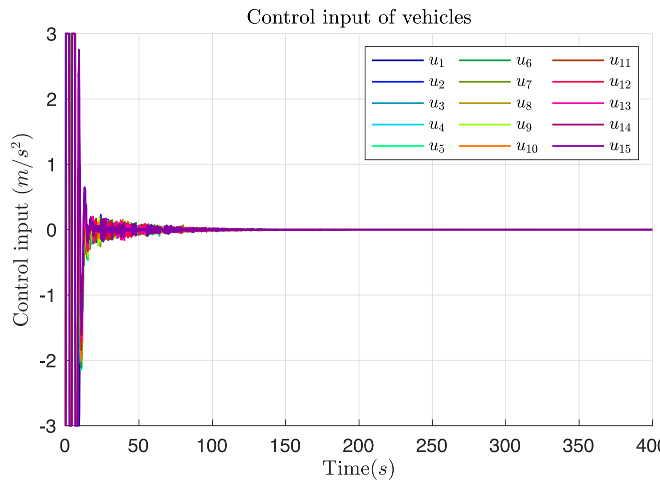

Fig. 1. Control inputs of vehicles.

Similarly, recalling (42) and (41), one has

$$\frac{z_{\text{sup},0k}}{g((k+1)T)} \leq \left(\frac{\rho_0}{\mathbf{e}^{\|\mathcal{A}_c\|T}} + \frac{\rho_0\rho_4\rho_5}{\|\Gamma\|}\right)\frac{b_0\sqrt{3N}\hbar\mathbf{e}^{\|\mathcal{A}_c\|T}}{\gamma} \triangleq c_2$$
$$\frac{\bar{z}_{\text{sup},k}}{g((k+1)T)} \leq a_4\frac{b_0\sqrt{3N}\hbar\mathbf{e}^{\|\mathcal{A}_c\|T}}{\gamma} \triangleq c_3.$$

Keeping the above inequalities in mind, one has that (49) is bounded and its upper bound is denoted as c_4, that is

$$\left\| \frac{\int_{kT}^{t}(\mathbf{e}^{\mathcal{A}_c(t-kT)})(I_N \otimes B)\tilde{u}(\tau)d\tau}{g((k+1)T)} \right\| \leq c_4. \quad (50)$$

Finally, by selecting $\gamma > \mathbf{e}^{(\vartheta/[2\lambda_{\max}(Q)])}$ and recalling (37), one has

$$\left\| \frac{\int_{kT}^{t} \mathbf{e}^{\mathcal{A}_c(t-kT)}Le_o(\tau)d\tau}{g((k+1)T)} \right\| \leq \frac{b_0\rho_5T\sqrt{3N}\hbar\mathbf{e}^{\|\mathcal{A}_c\|T}}{\gamma\|\Gamma\|} \triangleq c_5.$$

Combining the inequalities above, we can conclude that

$$\left\| \frac{\tilde{x}_i((k+1)T) - e^{\mathcal{A}_cT}\xi_i(kT)}{g((k+1)T)} \right\| \leq c \quad (51)$$

with $c = c_1 + c_4 + c_5$, which means $\|\Delta_i\|$ is bounded for time instant $t = (k+1)T$. Due to the arbitrariness of time instant k, the conclusion (51) always holds for all $k = 0, 1, 2, \ldots$ and the proof is therefore completed. ■

Remark 6: It should be pointed out that data privacy in the context of intelligent transportation systems mainly focuses on logical privacy and overlook the control problem of vehicular platoons [21], [22], [23], [24], [25]. Conversely, those who have considered the control issue fail to take into account the preservation of privacy [17], [18], [19]. The primary challenge lies in how to analyze privacy and platoon performance within a unified framework, and this article fills this gap. When considering vehicles with directed information flow topologies, our method, which is dependent on the specific structure of platooning error dynamics, converts the original platooning control problem into a stability problem of an auxiliary system such that the control gain design for the platoon only requires the maximum and minimum eigenvalues of the topology matrix. From the perspective of real application, this article examines actuator saturation (especially for the jerk limitation of vehicles), which reflects the requirement of the passenger's comfort [48].

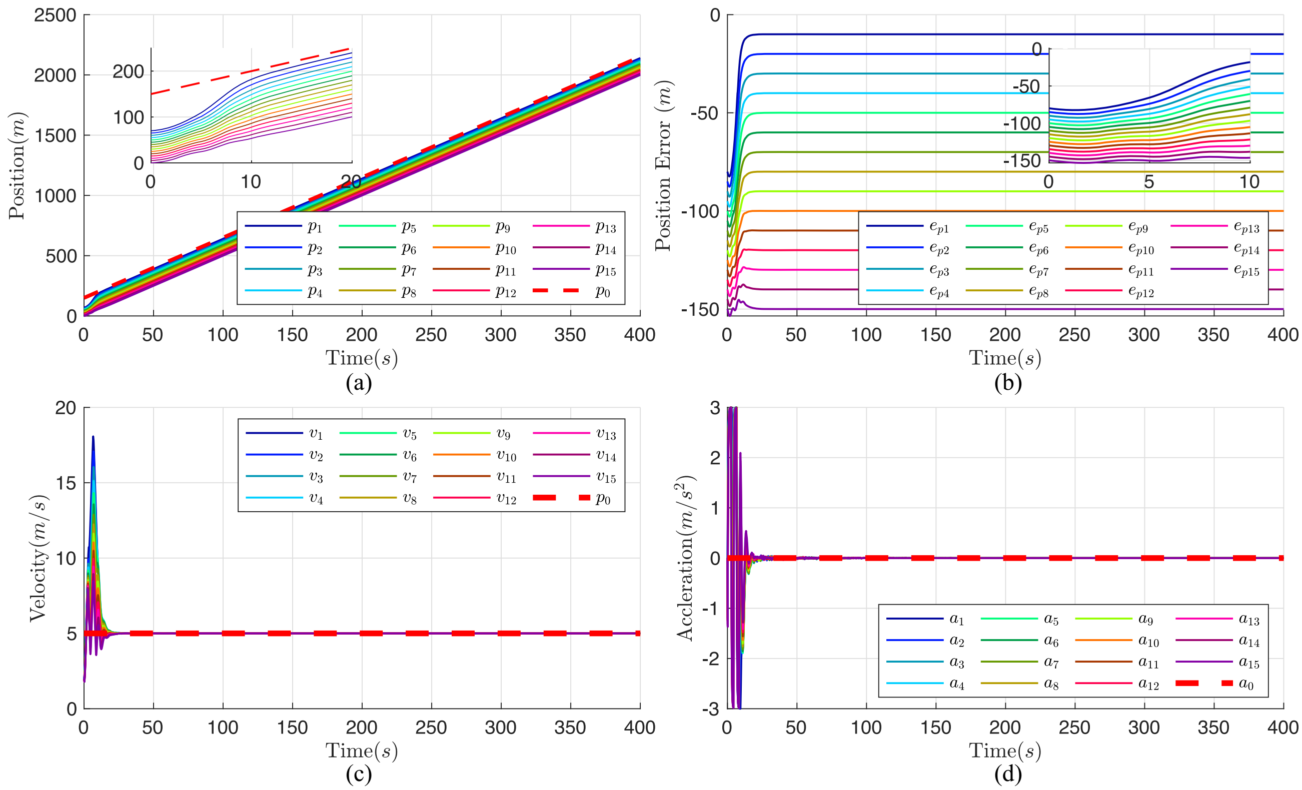

Fig. 2. Platoon behavior. (a) Position of vehicles. (b) Position errors. (c) Velocity of vehicles. (d) Acceleration of vehicles.

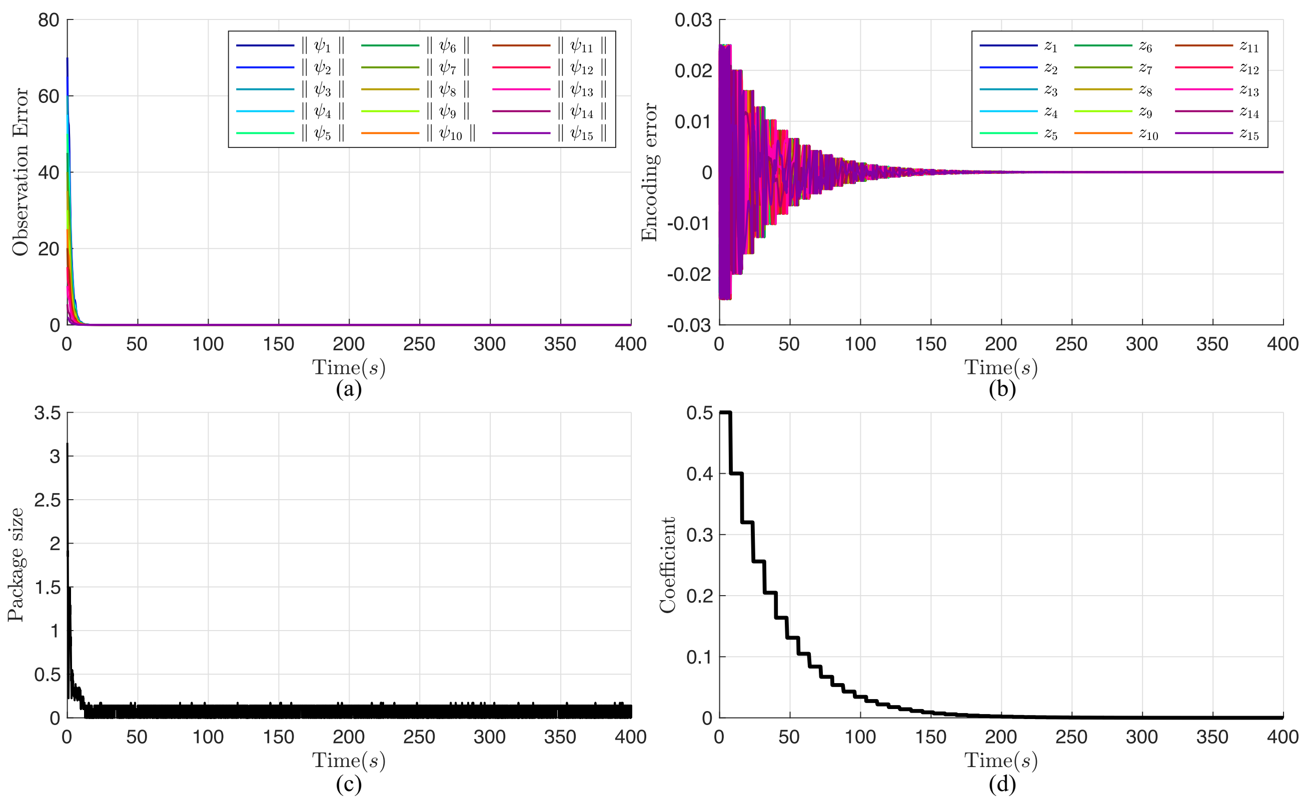

Fig. 3. Observer errors and evolutions of encryptors. (a) Overall observation error. (b) Encryption errors. (c) Maximum package size. (d) Dynamic private key.

IV. SIMULATIONS

In this section, an illustrative example is presented to demonstrate the efficacy and merits of the developed results. Without loss of generality, we consider a platoon consisting of 15 vehicles over a PF information flow topology (that is, each vehicle receives information from its direct predecessor).

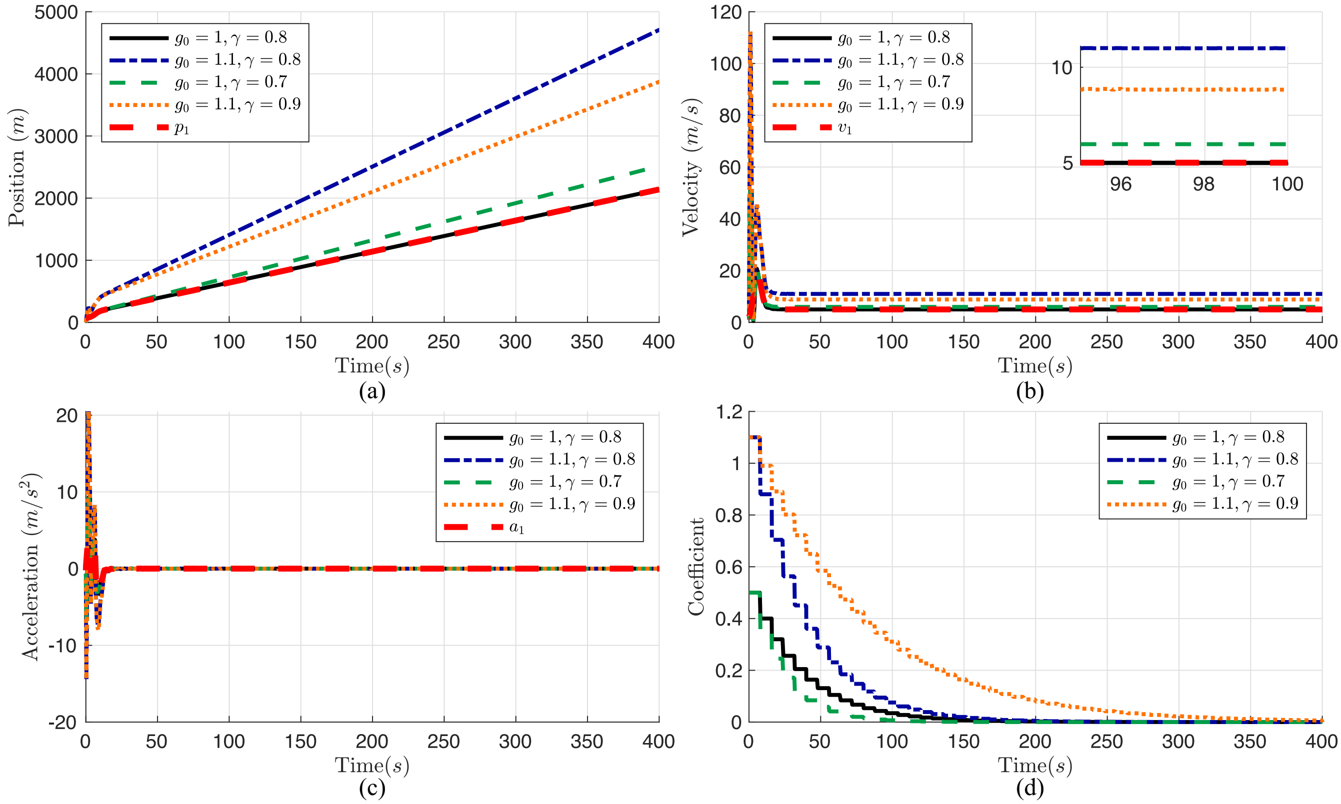

Fig. 4. Decrypted data by different private keys. (a) Decrypted position. (b) Decrypted velocity. (c) Decrypted acceleration. (d) Dynamic private keys.

The Inertial lag of vehicle engine dynamics is chosen as $\tau = 0.3$ s and it is assumed that only the position information can be measured, that is, the output matrix takes the form of $C = [1,\ 0,\ 0]$. The parameters in the dynamic private key, dependent on the desired capability of privacy preserving, are selected as $g_0 = 1$ and $\gamma = 0.8$. For the purpose of balancing the effect of quantization and privacy preservation, the quantization level is set to be $\hbar = 0.1$. Parameters $\eta = 0.03$ and $\epsilon_1 = 0.1$ are selected to satisfy the requirement of Young's inequalities, and parameter β is selected to be 0.9534. Furthermore, considering the physical limitation and the comfort of the passengers, the saturation value of the actuator is set to be $u_{\max} = 3$ m/s^2, and the corresponding scalar is set to be $\iota = 0.9246$. Sampling period T is set to be 0.01. Furthermore, solving the linear matrix inequalities in Theorems 1 and 2, we obtain the desired gains as $L_I = [1.1721,\ 0.5337,\ -0.3714]^\top$, $L_P = [1.2006,\ 2.4429,\ -3.2816]^\top$, and $K = [-0.7908,\ -2.9803,\ -0.9609]$. Finally, it is easily verified that the selected parameters satisfy the conditions in Theorem 2.

A. Platooning Control Performance Validation

Applying the designed PIOs and controllers, the relative simulation results are presented in Figs. 1–3. Specifically, Fig. 1 depicts the saturated control inputs implemented by each platoon vehicles. Fig. 2 plots the platoon behavior with PIO (4), encryptor (7), and decryptor (9). It can be observed that all following vehicles under the guidance of the leader move forward orderly and the desired safety spacing among vehicles is definitely guaranteed. Hence, the anticipated vehicular platooning control performance is successfully achieved even in the presence of input saturations and privacy preservation. Note that the abrupt changes of the control effort and platoon behavior at the initial stage in Figs. 1 and 2(d) arise from the effects of nonzero initial spacing and velocity errors as well as the input saturation. On the other hand, it is clear from Fig. 3(a) and (d) that observer errors converge to zero faster than the dynamic private key, which complies with the condition for Theorem 2. Fig. 3(c) and (d) indicate that although dynamic private key decreases over time, package size is always limited, which matches the conclusion of Theorem 3. Furthermore, one can see from Fig. 3(b) that encryption errors also converge to zero over time.

B. Privacy Preservation Performance Comparison

To examine the performance of our privacy preservation scheme, it is assumed that eavesdroppers are capable to acquire our encryption and decryption schemes and obtain all the transmitted vehicular data. However, they are not able to access the private key from each vehicle. As such, eavesdroppers have to employ unmatched dynamic private keys to decrypt the stolen data with four different parameters for the comparison: 1) $g_0 = 1$ and $\gamma = 0.8$; 2) $g_0 = 1.1$ and $\gamma = 0.8$; 3) $g_0 = 1$ and $\gamma = 0.7$; and 4) $g_0 = 1.1$ and $\gamma = 0.9$.

The decrypted results are given in Fig. 4, from which one can observe that: 1) eavesdroppers could obtain the actual states of the vehicle if they obtain the right key (i.e., $g_0 = 1$ and $\gamma = 0.8$) and 2) the decrypted states undoubtedly deviate from the actual ones as time goes if the wrong key is carried out. It is verified that the data privacy can be preserved as long as keeping the key private for eavesdroppers. Additionally, although γ is chosen as a number from the interval $(0, 1)$, there is no limitation on choosing $g_0 > 0$. Therefore, $g(t)$ can be any positive real scalar for eavesdroppers, which guarantees the privacy of the encrypted data.

V. Conclusion

This article investigated the distributed platooning control of vehicular cyber–physical systems with data privacy preservation and input saturation constraints. Considering that not all states of vehicles are obtainable, a distributed PIO was designed for each vehicle to estimate its unavailable full state at every instant of time. Different from traditional distributed observers, the integral term with a forgetting factor was adopted to achieve the tradeoff between transient performance and steady-state performance. Then, distributed sampled-data-based encryptors and decryptors with a dynamic private key were designed to encrypt and decrypt the estimated states on each platoon vehicle, which were further employed to generate the desired control inputs. After that, the platooning control issue was creatively transformed into the general stability issue of an auxiliary system. Sufficient conditions involving the selected range of parameters in private keys were derived to guarantee the desired platoon stability and privacy preservation performance. One of our future work will focus on platooning control with simultaneous privacy-preserving and collision-free guarantees [49], [50].

References

[1] L. Li, Y. Lin, N. Zheng, and F.-Y. Wang, "Parallel learning: A perspective and a framework," *IEEE/CAA J. Automatica Sinica*, vol. 4, no. 3, pp. 389–395, Jul. 2017.

[2] L. Li, Y. Lin, D. Cao, N. Zheng, and F.-Y. Wang, "Parallel learning—A new framework for machine learning," *Acta Automatica Sinica*, vol. 43, no. 1, pp. 1–8, 2017.

[3] F.-Y. Wang, "MetaVehicles in the metaverse: Moving to a new phase for intelligent vehicles and smart mobility," *IEEE Trans. Intell. Veh.*, vol. 7, no. 1, pp. 1–5, Mar. 2022.

[4] Q. Wei, H. Li, and F.-Y. Wang, "Parallel control for continuous-time linear systems: A case study," *IEEE/CAA J. Automatica Sinica*, vol. 7, no. 4, pp. 919–928, Jul. 2020.

[5] G. Fortino, F. Messina, D. Rosaci, and G. M. L. Sarne, "ResIoT: An IoT social framework resilient to malicious activities," *IEEE/CAA J. Automatica Sinica*, vol. 7, no. 5, pp. 1263–1278, Sep. 2020.

[6] F.-Y. Wang, Y. Li, W. Zhang, G. Bennett, and N. Chen, "Digital twin and parallel intelligence based on location and transportation: A vision for new synergy between the IEEE CRFID and ITSS in cyberphysical social systems," *IEEE Intell. Transp. Syst. Mag.*, vol. 13, no. 1, pp. 249–252, Jan. 2021.

[7] T. Liu, Y. Xing, X. Tang, H. Wang, H. Yu, and F.-Y. Wang, "Cyber-physical-social system for parallel driving: From concept to application," *IEEE Intell. Transp. Syst. Mag.*, vol. 13, no. 1, pp. 59–69, Sep. 2021.

[8] J. Cao, S. Wang, B. Li, X. Wang, Z. Ding, and F.-Y. Wang, "Integrating multisourced texts in online business intelligence systems," *IEEE Trans. Syst., Man, Cybern., Syst.*, vol. 50, no. 5, pp. 1638–1648, May 2020.

[9] M. Al-Sharman et al., "A sensorless state estimation for a safety-oriented cyber-physical system in urban driving: Deep learning approach," *IEEE/CAA J. Automatica Sinica*, vol. 8, no. 1, pp. 169–178, Jan. 2021.

[10] J. Nie, J. Yan, H. Yin, L. Ren, and Q. Meng, "A multimodality fusion deep neural network and safety test strategy for intelligent vehicles," *IEEE Trans. Intell. Veh.*, vol. 6, no. 2, pp. 310–322, Jun. 2021.

[11] A. Amini, A. Asif, and A. Mohammadi, "RQ-CEASE: A resilient quantized collaborative event-triggered average-consensus sampled-data framework under denial of service attack," *IEEE Trans. Syst., Man, Cybern., Syst.*, vol. 51, no. 11, pp. 7027–7039, Nov. 2021.

[12] M. Fanti, A. Mangini, A. Favenza, and G. Difilippo, "An eco-route planner for heavy duty vehicles," *IEEE/CAA J. Automatica Sinica*, vol. 8, no. 1, pp. 37–51, Jan. 2021.

[13] S. Feng, Y. Zhang, S. E. Li, Z. Cao, H. X. Liu, and L. Li, "String stability for vehicular platoon control: Definitions and analysis methods," *Annu. Rev. Control*, vol. 47, pp. 81–97, Mar. 2019.

[14] X. Ge, Q.-L. Han, L. Ding, Y.-L. Wang, and X.-M. Zhang, "Dynamic event-triggered distributed coordination control and its applications: A survey of trends and techniques," *IEEE Trans. Syst., Man, Cybern., Syst.*, vol. 50, no. 9, pp. 3112–3125, Sep. 2020.

[15] S. Feng, Z. Song, Z. Li, Y. Zhang, and L. Li, "Robust platoon control in mixed traffic flow based on tube model predictive control," *IEEE Trans. Intell. Veh.*, vol. 6, no. 4, pp. 711–722, Dec. 2021.

[16] V. Lesch, M. Breitbach, M. Segata, C. Becker, S. Kounev, and C. Krupitzer, "An overview on approaches for coordination of platoons," *IEEE Trans. Intell. Transp. Syst.*, vol. 23, no. 8, pp. 10049–10065, Aug. 2022.

[17] Y. Li, C. Tang, K. Li, S. Peeta, X. He, and Y. Wang, "Nonlinear finite-time consensus-based connected vehicle platoon control under fixed and switching communication topologies," *Transp. Res. C, Emerg. Technol.*, vol. 93, pp. 525–543, Aug. 2018.

[18] Y. Zheng, S. E. Li, J. Wang, D. Cao, and K. Li, "Stability and scalability of homogeneous vehicular platoon: Study on the influence of information flow topologies," *IEEE Trans. Intell. Transp. Syst.*, vol. 17, no. 1, pp. 14–26, Jan. 2016.

[19] B. Besselink et al., "Cyber–physical control of road freight transport," *Proc. IEEE*, vol. 104, no. 5, pp. 1128–1141, May 2016.

[20] D. Jia, K. Lu, J. Wang, X. Zhang, and X. Shen, "A survey on platoon-based vehicular cyber-physical systems," *IEEE Commun. Surveys Tuts.*, vol. 18, no. 1, pp. 263–284, 1st Quart., 2016.

[21] C. Chen, T. Xiao, T. Qiu, N. Lv, and Q. Pei, "Smart-contract-based economical platooning in blockchain-enabled urban Internet of Vehicles," *IEEE Trans. Ind. Informat.*, vol. 16, no. 6, pp. 4122–4133, Jun. 2020.

[22] R. Kumar, P. Kumar, R. Tripathi, G. P. Gupta, N. Kumar, and M. M. Hassan, "A privacy-preserving-based secure framework using blockchain-enabled deep-learning in cooperative intelligent transport system," *IEEE Trans. Intell. Transp. Syst.*, vol. 23, no. 9, pp. 16492–16503, Sep. 2022.

[23] M. A. Khan et al., "A provable and privacy-preserving authentication scheme for UAV-enabled intelligent transportation systems," *IEEE Trans. Ind. Informat.*, vol. 18, no. 5, pp. 3416–3425, May 2022.

[24] C. Zhang et al., "TPPR: A trust-based and privacy-preserving platoon recommendation scheme in VANET," *IEEE Trans. Services Comput.*, vol. 15, no. 2, pp. 806–818, Mar./Apr. 2022.

[25] L. Weng, L. Amsaleg, A. Morton, and S. Marchand-Maillet, "A privacy-preserving framework for large-scale content-based information retrieval," *IEEE Trans. Inf. Forensics Security*, vol. 10, pp. 152–167, 2015.

[26] Y. Xu, M. Fang, Z.-G. Wu, Y.-J. Pan, M. Chadli, and T. Huang, "Input-based event-triggering consensus of multiagent systems under denial-of-service attacks," *IEEE Trans. Syst., Man, Cybern., Syst.*, vol. 50, no. 4, pp. 1455–1464, Apr. 2020.

[27] S. Hu, D. Yue, X. Chen, Z. Cheng, and X. Xie, "Resilient H_∞ filtering for event-triggered networked systems under nonperiodic DoS jamming attacks," *IEEE Trans. Syst., Man, Cybern., Syst.*, vol. 51, no. 3, pp. 1392–1403, Mar. 2021.

[28] J. Liu, Z.-G. Wu, D. Yue, and J. H. Park, "Stabilization of networked control systems with hybrid-driven mechanism and probabilistic cyber attacks," *IEEE Trans. Syst., Man, Cybern., Syst.*, vol. 51, no. 2, pp. 943–953, Feb. 2021.

[29] J.-H. Cho et al., "Toward proactive, adaptive defense: A survey on moving target defense," *IEEE Commun. Surveys Tuts.*, vol. 22, no. 1, pp. 709–745, 1st Quart., 2020.

[30] H. Mun, M. Seo, and D. H. Lee, "Secure privacy-preserving V2V communication in 5G-V2X supporting network slicing," *IEEE Trans. Intell. Transp. Syst.*, vol. 23, no. 9, pp. 14439–14455, Sep. 2022.

[31] Y. Mo and R. M. Murray, "Privacy preserving average consensus," *IEEE Trans. Autom. Control*, vol. 62, no. 2, pp. 753–765, Feb. 2017.

[32] E. Nozari, P. Tallapragada, and J. Cortés, "Differentially private average consensus: Obstructions, trade-offs, and optimal algorithm design," *Automatica*, vol. 81, pp. 221–231, Jul. 2017.

[33] C. Zhao, J. He, P. Chen, and J. Chen, "Privacy-preserving consensus-based energy management in smart grid," *IEEE Trans. Signal Process.*, vol. 66, no. 23, pp. 6162–6176, Dec. 2018.
[34] C. Gao, Z. Wang, X. He, and D. Yue, "Sampled-data-based fault-tolerant consensus control for multi-agent systems: A data privacy preserving scheme," *Automatica*, vol. 133, Nov. 2021, Art no. 109847.
[35] C. Gao, Z. Wang, X. He, and H. Dong, "Fault-tolerant consensus control for multiagent systems: An encryption-decryption scheme," *IEEE Trans. Autom. Control*, vol. 67, no. 5, pp. 2560–2567, May 2022.
[36] X. Ge, S. Xiao, Q.-L. Han, X.-M. Zhang, and D. Ding, "Dynamic event-triggered scheduling and platooning control co-design for automated vehicles over vehicular ad-hoc networks," *IEEE/CAA J. Automatica Sinica*, vol. 9, no. 1, pp. 31–46, Jan. 2022.
[37] J. Xu, C. C. Mi, B. Cao, J. Deng, Z. Chen, and S. Li, "The state of charge estimation of lithium-ion batteries based on a proportional-integral observer," *IEEE Trans. Veh. Technol.*, vol. 63, no. 4, pp. 1614–1621, May 2014.
[38] D. Zhao, Z. Wang, Y. Chen, and G. Wei, "Proportional-integral observer design for multidelayed sensor-saturated recurrent neural networks: A dynamic event-triggered protocol," *IEEE Trans. Cybern.*, vol. 50, no. 11, pp. 4619–4632, Nov. 2020.
[39] S. Xiao, X. Ge, Q.-L. Han, and Y. Zhang, "Secure and collision-free multi-platoon control of automated vehicles under data falsification attacks," *Automatica*, vol. 145, Nov. 2022, Art. no. 110531.
[40] A. T. Al Ghazo, M. Ibrahim, H. Ren, and R. Kumar, "A2G2V: Automatic attack graph generation and visualization and its applications to computer and SCADA networks," *IEEE Trans. Syst., Man, Cybern., Syst.*, vol. 50, no. 10, pp. 3488–3498, Oct. 2020.
[41] H. Sun, C. Peng, D. Yue, Y. Wang, and T. Zhang, "Resilient load frequency control of cyber-physical power systems under QoS-dependent event-triggered communication," *IEEE Trans. Syst., Man, Cybern., Syst.*, vol. 51, no. 4, pp. 2113–2122, Apr. 2021.
[42] L. Xiong, N. Xiong, C. Wang, X. Yu, and M. Shuai, "An efficient lightweight authentication scheme with adaptive resilience of asynchronization attacks for wireless sensor networks," *IEEE Trans. Syst., Man, Cybern., Syst.*, vol. 51, no. 9, pp. 5626–5638, Sep. 2021.
[43] L. Wang, Z. Wang, B. Shen, and G. Wei, "Recursive filtering with measurement fading: A multiple description coding scheme," *IEEE Trans. Autom. Control*, vol. 66, no. 11, pp. 5144–5159, Nov. 2021.
[44] N. Zhao, P. Shi, W. Xing, and R. K. Agarwal, "Resilient event-triggered control for networked cascade control systems under denial-of-service attacks and actuator saturation," *IEEE Syst. J.*, vol. 16, no. 1, pp. 1114–1122, Mar. 2022.
[45] G. Guo and D. Li, "Adaptive sliding mode control of vehicular platoons with prescribed tracking performance," *IEEE Trans. Veh. Technol.*, vol. 68, no. 8, pp. 7511–7520, Aug. 2019.
[46] R. Hoek, J. Ploeg, and H. Nijmeijer, "Cooperative driving of automated vehicles using B-splines for trajectory planning," *IEEE Trans. Intell. Veh.*, vol. 6, no. 3, pp. 594–604, Sep. 2021.
[47] L. Sun, Y. Wang, and G. Feng, "Control design for a class of affine nonlinear descriptor systems with actuator saturation," *IEEE Trans. Autom. Control*, vol. 60, no. 8, pp. 2195–2200, Aug. 2015.
[48] A. Scamarcio, M. Metzler, P. Gruber, S. De Pinto, and A. Sorniotti, "Comparison of anti-jerk controllers for electric vehicles with on-board motors," *IEEE Trans. Veh. Technol.*, vol. 69, no. 10, pp. 10681–10699, Oct. 2020.
[49] M. Parseh, F. Asplund, L. Svensson, W. Sinz, E. Tomasch, and M. Törngren, "A data-driven method towards minimizing collision severity for highly automated vehicles," *IEEE Trans. Intell. Veh.*, vol. 6, no. 3, pp. 723–735, Dec. 2021.
[50] B. Fan and X. Wang, "Distributed privacy-preserving active power sharing and frequency regulation in microgrids," *IEEE Trans. Smart Grid*, vol. 12, no. 4, pp. 3665–3668, Jul. 2021.

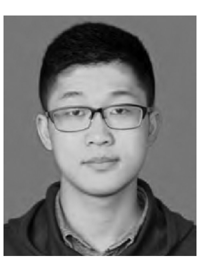

Dengfeng Pan received the B.Sc. degree in network engineering from Jianghan University, Wuhan, China, in 2018, and the M.Sc. degree in control engineering from Jiangnan University, Wuxi, China. He is currently pursuing the Ph.D. degree in control engineering with the Swinburne University of Technology, Melbourne, VIC, Australia.

His research interests include intelligent transportation systems and data privacy preservation.

Derui Ding (Senior Member, IEEE) received the B.Sc. degree in industry engineering and the M.Sc. degree in detection technology and automation equipment from Anhui Polytechnic University, Wuhu, China, in 2004 and 2007, respectively, and the Ph.D. degree in control theory and control engineering from Donghua University, Shanghai, China, in 2014.

He is currently a Senior Research Fellow with the School of Science, Computing and Engineering Technologies, Swinburne University of Technology, Melbourne, VIC, Australia. He was a Teaching Assistant and then a Lecturer with the Department of Mathematics, Anhui Polytechnic University from July 2007 to December 2014. He was a Research Assistant with the Department of Mechanical Engineering, The University of Hong Kong, Hong Kong, from June 2012 to September 2012. He was a Visiting Scholar with the Department of Information Systems and Computing, Brunel University London, London, U.K., from March 2013 to March 2014. He was a Research Assistant with the Department of Mathematics, City University of Hong Kong, Hong Kong, from June 2015 to August 2015. His research interests include nonlinear stochastic control and filtering, as well as distributed control, and filtering and optimization.

Dr. Ding is an Associate Editor of the *Neurocomputing* and *IET Control Theory & Applications*, and an Early Career Advisory Board Member of the IEEE/CAA JOURNAL OF AUTOMATICA SINICA. He also served as a Guest Editor for several issues, including the *Information Sciences*, *International Journal of Systems Science*, and *International Journal of General Systems*.

Xiaohua Ge (Senior Member, IEEE) received the Ph.D. degree in computer engineering from Central Queensland University, Rockhampton, QLD, Australia, in 2014.

He was a Research Fellow with the Griffith School of Engineering, Griffith University, Gold Coast, QLD, Australia, from 2015 to 2017. He is currently a Senior Lecturer with the School of Science, Computing and Engineering Technologies, Swinburne University of Technology, Melbourne, VIC, Australia. His research interests include networked, secure, and intelligent control and estimation theories, and their applications in electric vehicles, intelligent robotic vehicles, connected automated vehicles, and intelligent transportation systems.

Dr. Ge is an Associate Editor of the IEEE TRANSACTIONS ON SYSTEMS, MAN, AND CYBERNETICS: SYSTEMS, IEEE TRANSACTIONS ON INTELLIGENT VEHICLES, and IEEE TRANSACTIONS ON CIRCUITS AND SYSTEMS—PART II: EXPRESS BRIEFS. He serves as an Early Career Advisory Board Member of the IEEE/CAA JOURNAL OF AUTOMATICA SINICA.

Qing-Long Han (Fellow, IEEE) received the B.Sc. degree in mathematics from Shandong Normal University, Jinan, China, in 1983, and the M.Sc. and Ph.D. degrees in control engineering from the East China University of Science and Technology, Shanghai, China, in 1992 and 1997, respectively.

He is a Pro Vice-Chancellor (Research Quality) and a Distinguished Professor with the Swinburne University of Technology, Melbourne, VIC, Australia. He held various academic and management positions with Griffith University, Gold Coast, QLD, Australia, and Central Queensland University, Rockhampton, QLD, Australia. His research interests include networked control systems, multiagent systems, time-delay systems, smart grids, unmanned surface vehicles, and neural networks.

Prof. Han was awarded the 2021 Norbert Wiener Award (the Highest Award in systems science and engineering, and cybernetics) and the 2021 M. A. Sargent Medal (the Highest Award of the Electrical College Board of Engineers Australia). He was the recipient of the 2022 IEEE Systems, Man, and Cybernetics Society Andrew P. Sage Best Transactions Paper Award, the 2021 IEEE/CAA JOURNAL OF AUTOMATICA SINICA Norbert Wiener Review Award, the 2020 IEEE Systems, Man, and Cybernetics Society Andrew P. Sage Best Transactions Paper Award, the 2020 IEEE TRANSACTIONS ON INDUSTRIAL INFORMATICS Outstanding Paper Award, and the 2019 IEEE Systems, Man, and Cybernetics Society Andrew P. Sage Best Transactions Paper Award. He is a member of the Academia Europaea (The Academy of Europe). He is a Highly Cited Researcher in both Engineering and Computer Science (Clarivate). He has served as an AdCom Member of IEEE Industrial Electronics Society (IES), a member of the IEEE IES Fellows Committee and IEEE IES Publications Committee, and the Chair of IEEE IES Technical Committee on Networked Control Systems. He is the Editor-in-Chief of the IEEE/CAA JOURNAL OF AUTOMATICA SINICA, the Co-Editor-in-Chief of the IEEE TRANSACTIONS ON INDUSTRIAL INFORMATICS, and a Co-Editor of the *Australian Journal of Electrical and Electronic Engineering*. He is a Fellow of the International Federation of Automatic Control and the Institution of Engineers Australia.

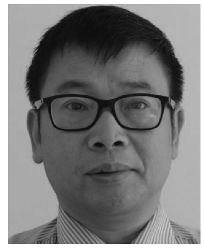

Xian-Ming Zhang (Senior Member, IEEE) received the M.Sc. degree in applied mathematics and the Ph.D. degree in control theory and control engineering from Central South University, Changsha, China, in 1992 and 2006, respectively.

In 1992, he joined Central South University, where he was an Associate Professor with the School of Mathematics and Statistics. He was a Postdoctoral Research Fellow and a Lecturer with the School of Engineering and Technology, Central Queensland University, Rockhampton, QLD, Australia, from 2007 to 2014. He was a Lecturer with the Griffith School of Engineering, Griffith University, Gold Coast, QLD, Australia, from 2014 to 2016. He joined the Swinburne University of Technology, Melbourne, VIC, Australia, in 2016, where he is currently an Associate Professor with the School of Science, Computing and Engineering Technologies. His current research interests include H-infinity filtering, event-triggered control systems, networked control systems, neural networks, multiagent systems, offshore platforms, and time-delay systems.

Prof. Zhang was a recipient of the Second National Natural Science Award in China in 2013, jointly with Prof. M. Wu and Prof. Y. He. He was also the recipient of the 2020 IEEE TRANSACTIONS ON INDUSTRIAL INFORMATICS Outstanding Paper Award, the 2019 IEEE Systems, Man, and Cybernetics Society Andrew P. Sage Best Transactions Paper Award, and the 2016, 2020 IET Control Theory and Applications Premium Award. He is an Associate Editor of the IEEE TRANSACTIONS ON CYBERNETICS, *IET-Control Theory & Applications*, *Journal of the Franklin Institute*, *International Journal of Control, Automation, and Systems*, *Neurocomputing*, and *Neural Processing Letters*.